

Deformed Halo Nuclei ~ theoretical aspects ~

Kouichi Hagino
Tohoku University

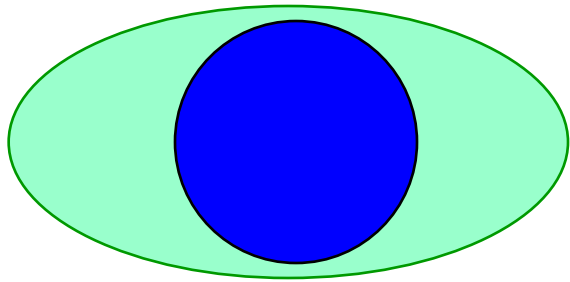


- 1. Deformed halo nucleus: what is it?*
- 2. Single-particle motion in a deformed potential*
- 3. Particle-rotor model and its application to ^{31}Ne*
- 4. $2n$ halo nuclei: odd-even staggering of σ_R
and pairing correlation*
- 5. Summary*

What is “deformed halo”? : definition

halo: core-valence decoupling

halo + deformation:



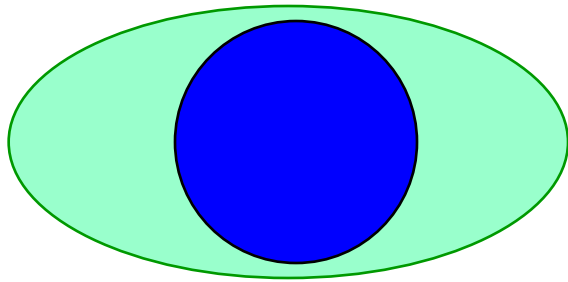
spherical core
+ deformed valence
orbit

cf. ^{17}O : slightly oblate

What is “deformed halo”? : definition

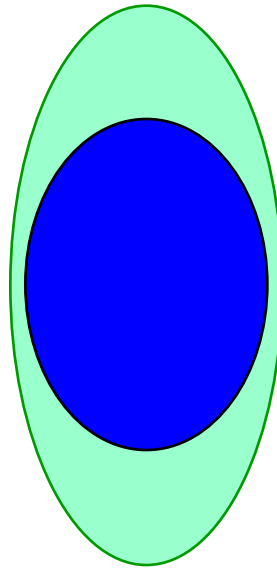
halo: core-valence decoupling

halo + deformation:

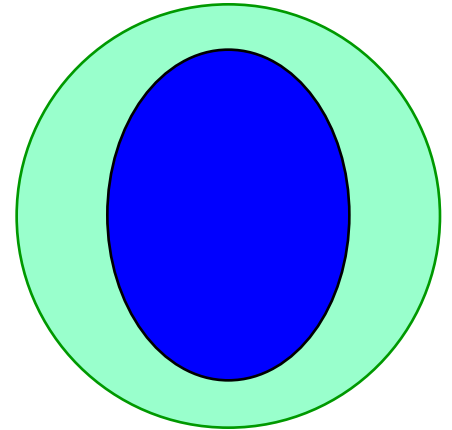


spherical core
+ deformed valence
orbit

cf. ^{17}O : slightly oblate



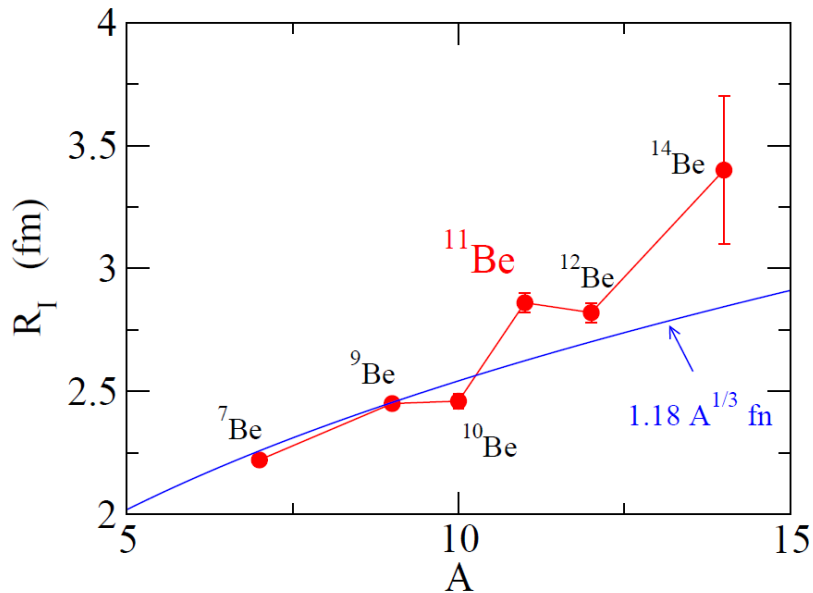
deformed core
+ def. orbit



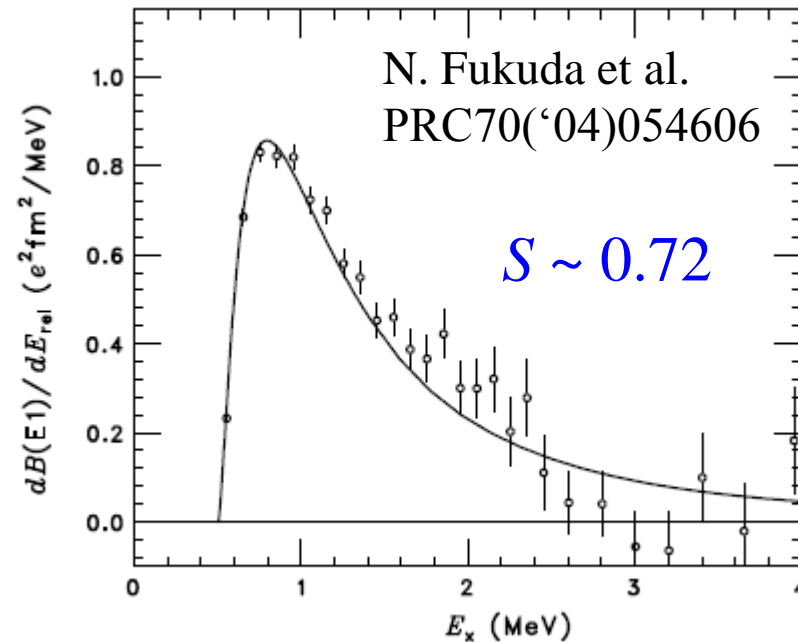
deformed core
+ spherical orbit

deformed halo nucleus

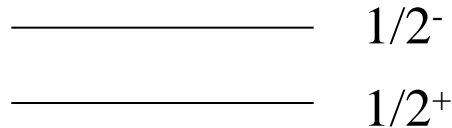
Well-known example: ^{11}Be ($S_n = 504 \pm 6 \text{ keV}$)



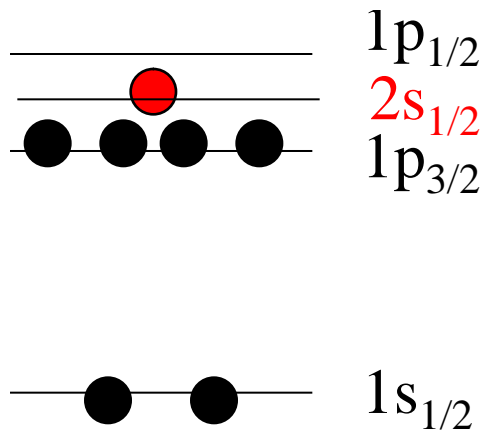
I. Tanihata et al.,
PRL55('85)2676; PLB206('88)592



0.32 MeV



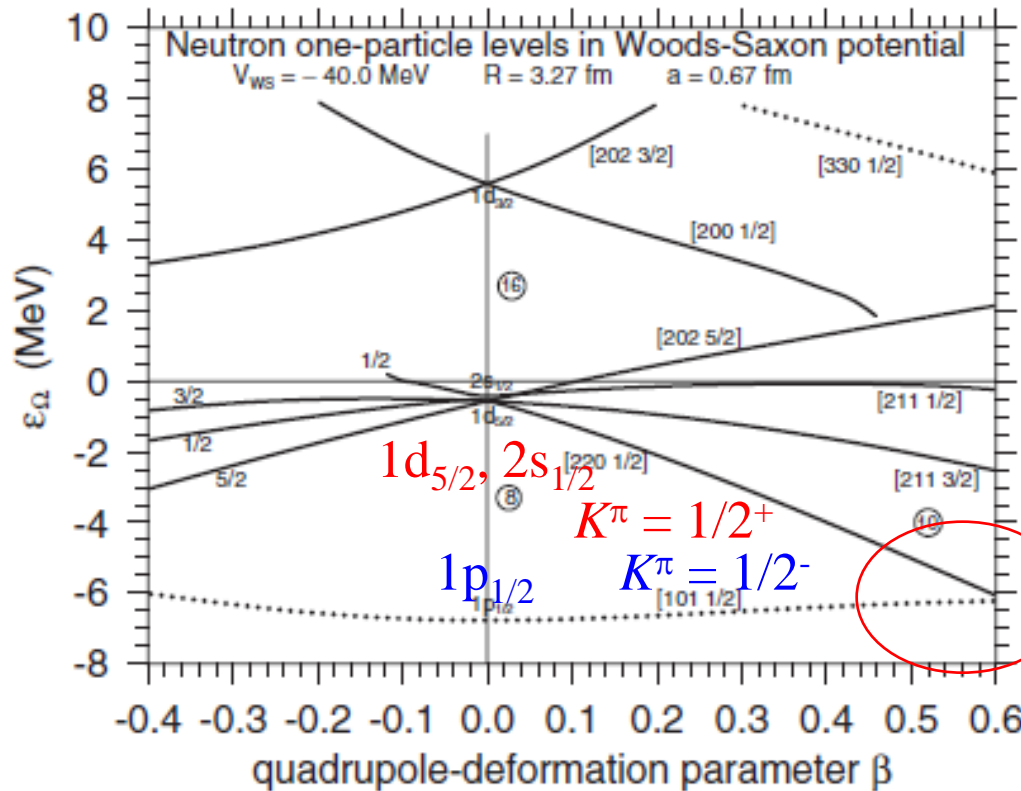
^{11}Be



“parity inversion”

deformed ^{11}Be ? \longrightarrow single-particle motion in a deformed potential

Can deformation effect explain the level scheme of ^{11}Be ?



← inversion of + parity and - parity states at large deformation

I. Hamamoto, J. Phys. G37('10)055102

cf. coupled-channels calculation with finite core excitation energies:

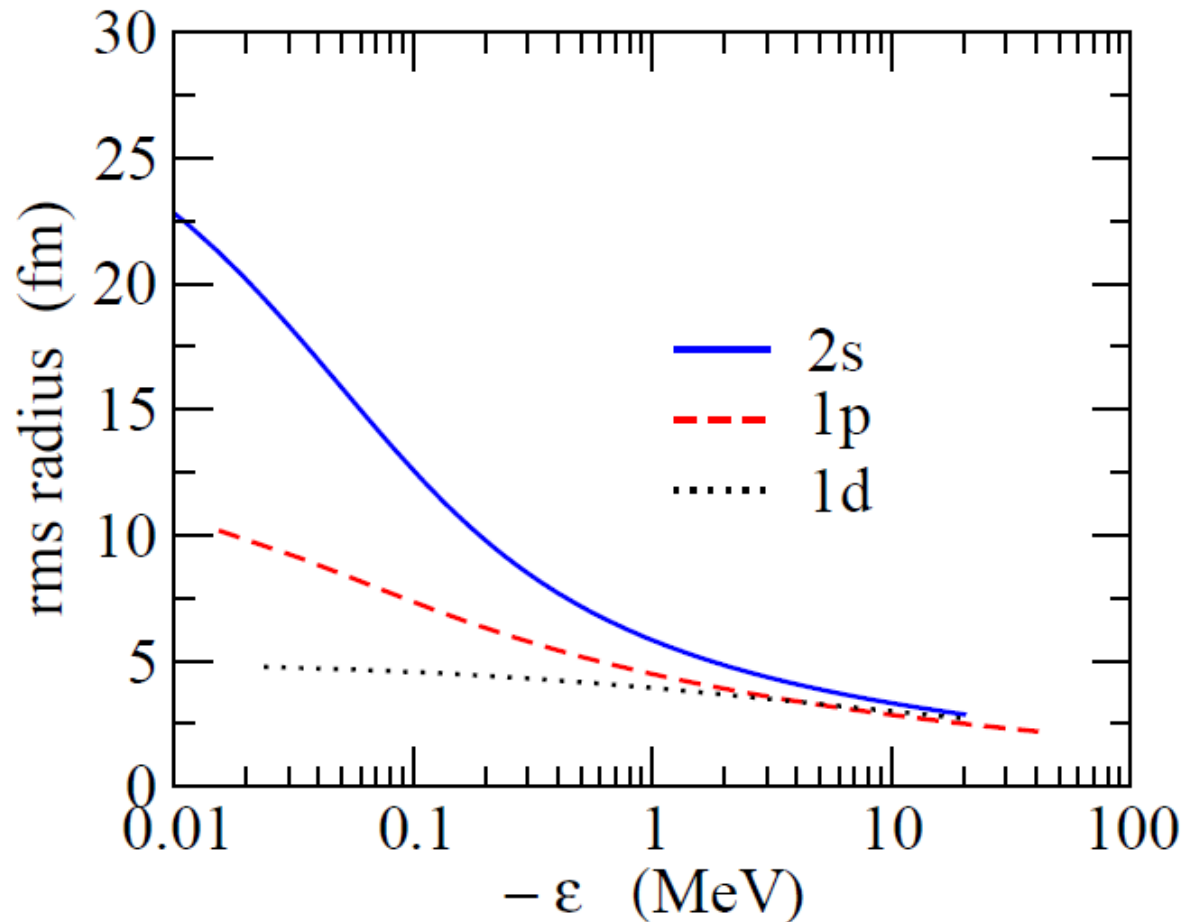
H. Esbensen, B.A. Brown, H. Sagawa, PRC51('95)1274

F.M. Nunes, I.J. Thompson, R.C. Johnson, NPA596('96)171

Role of s.p. angular momentum in halo formation

$$\langle r^2 \rangle \propto \begin{array}{ll} 1/|\epsilon_0| & (l = 0) \\ 1/\sqrt{|\epsilon_1|} & (l = 1) \\ \text{const.} & (l = 2) \end{array}$$

K. Riisager,
A.S. Jensen, and
P. Moller, NPA548('92)393



radius: diverges for $l = 0, 1$
in the zero binding limit

halo (anomalously large
radius): $l = 0$ or 1

s.p. motion in a deformed potential

halo : only for $l = 0$ or 1

⇒ however, a possibility is enlarged for a deformed nucleus

deformed potential $V(r, \theta)$ → mixture of angular momenta

e.g.,

$$|d_{5/2}\rangle \rightarrow |d_{5/2}\rangle + |s_{1/2}\rangle + |g_{7/2}\rangle + \dots$$

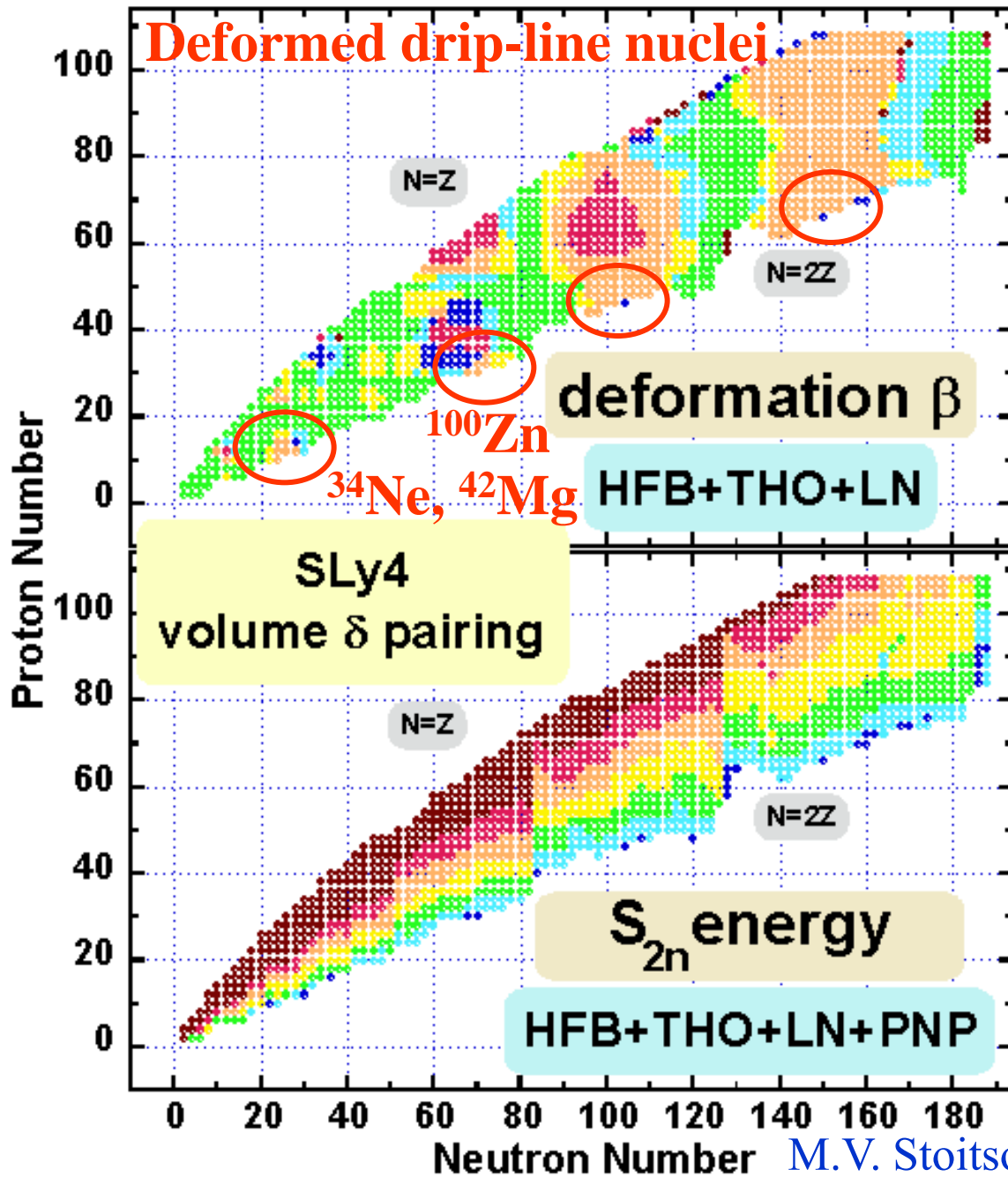
$$|f_{7/2}\rangle \rightarrow |f_{7/2}\rangle + |p_{3/2}\rangle + |p_{1/2}\rangle + \dots$$

(note) $s_{1/2} : \Omega^\pi = 1/2^+$ only

$p_{1/2} : \Omega^\pi = 1/2^-$ only

$p_{3/2} : \Omega^\pi = 3/2^-$ and $1/2^-$ only

} → possibility of halo
only for s.p. states
with
 $\Omega^\pi = 1/2^+, 1/2^-, 3/2^-$



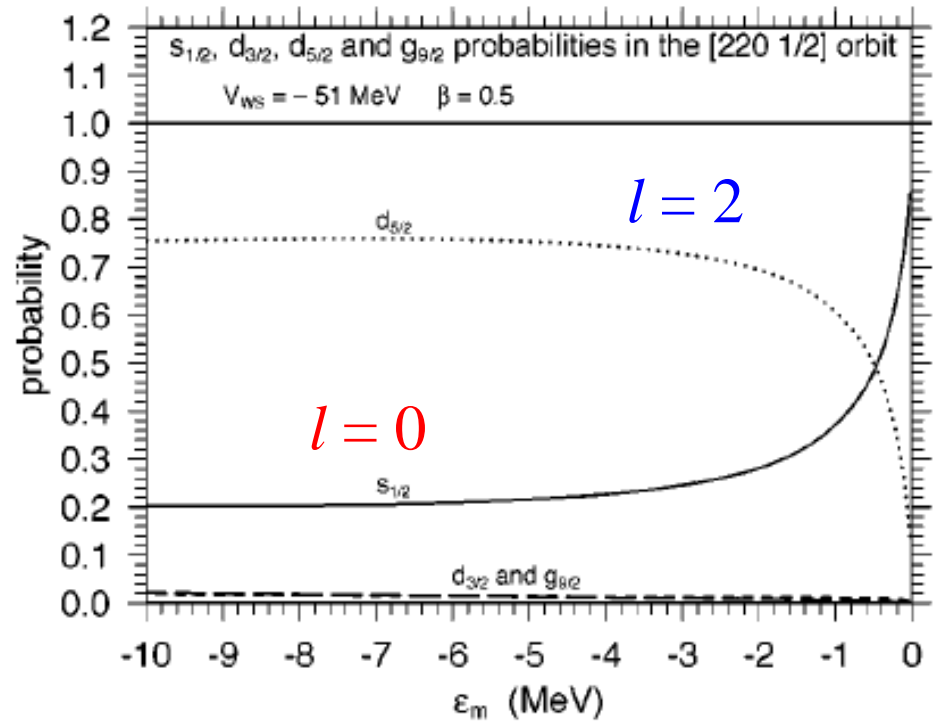
^{32}Ne :
 $\beta=0.151$
 ^{34}Ne :
 $\beta=0.277$
 ^{42}Mg :
 $\beta=-0.18$
 ^{100}Zn :
 $\beta=0.244$



s.p. motion in a deformed potential

$$\begin{aligned} |d_{5/2}\rangle &\rightarrow |d_{5/2}\rangle + |s_{1/2}\rangle + |g_{7/2}\rangle + \dots \\ &\rightarrow |s_{1/2}\rangle \quad (|\epsilon| \rightarrow 0) \end{aligned}$$

T. Misu, W. Nazarewicz,
and S. Aberg, NPA614('97)44
(deformed square well)



I. Hamamoto, PRC69('04)041306(R)
(deformed Woods-Saxon)

reason for s-wave dominance

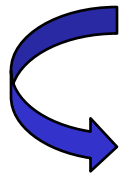
$$\Psi(\mathbf{r}) = \sum_l R_l(r) Y_{lK}(\hat{\mathbf{r}}) \equiv \sum_l \psi_{lK}(\mathbf{r})$$

$$P_l = \frac{\langle \psi_{lK} | \psi_{lK} \rangle}{\langle \Psi | \Psi \rangle} = \frac{\langle \psi_{lK} | \psi_{lK} \rangle}{\sum_{l'} \langle \psi_{l'K} | \psi_{l'K} \rangle}$$

(note)

$$\langle \psi_{lK} | \psi_{lK} \rangle$$

diverges for $l = 0$ ($\epsilon \rightarrow 0$)
finite for $l > 0$

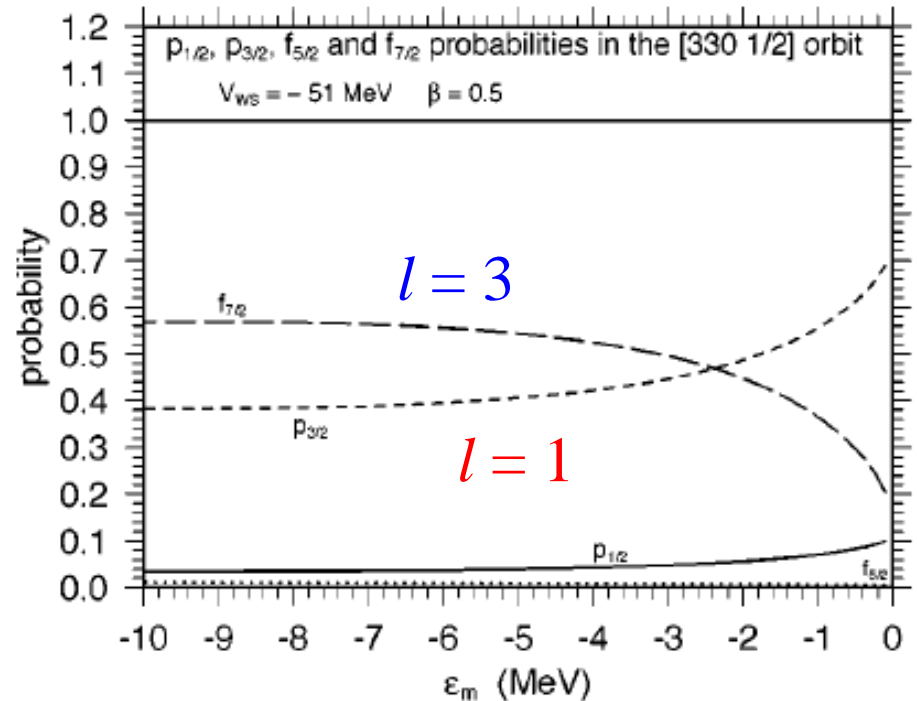
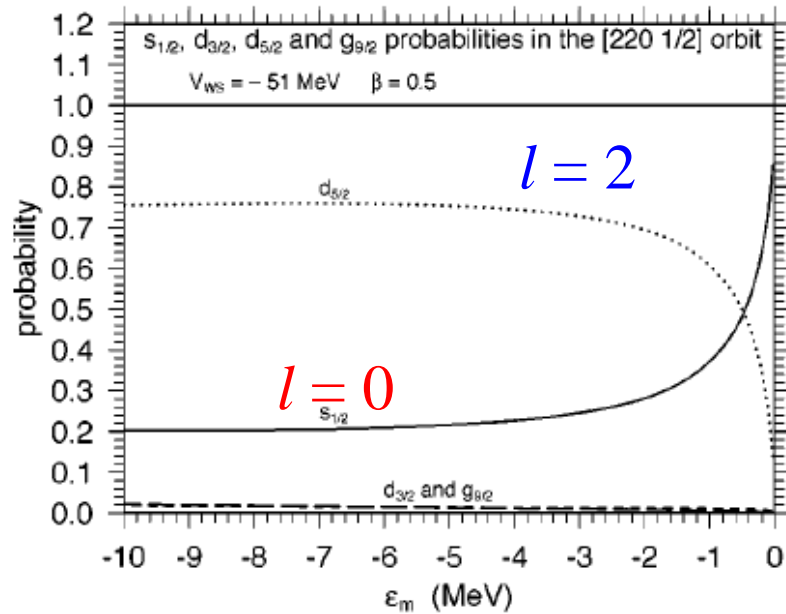


$$P_l \sim \frac{\langle \psi_{lK} | \psi_{lK} \rangle}{\langle \psi_{0K} | \psi_{0K} \rangle} = 1 \quad (l = 0)$$

(note)

$$\beta_2 \propto \frac{\langle r^2 Y_{20} \rangle}{\langle r^2 \rangle} \rightarrow 0 \quad (\epsilon \rightarrow 0)$$

similar dominance phenomenon for p -wave



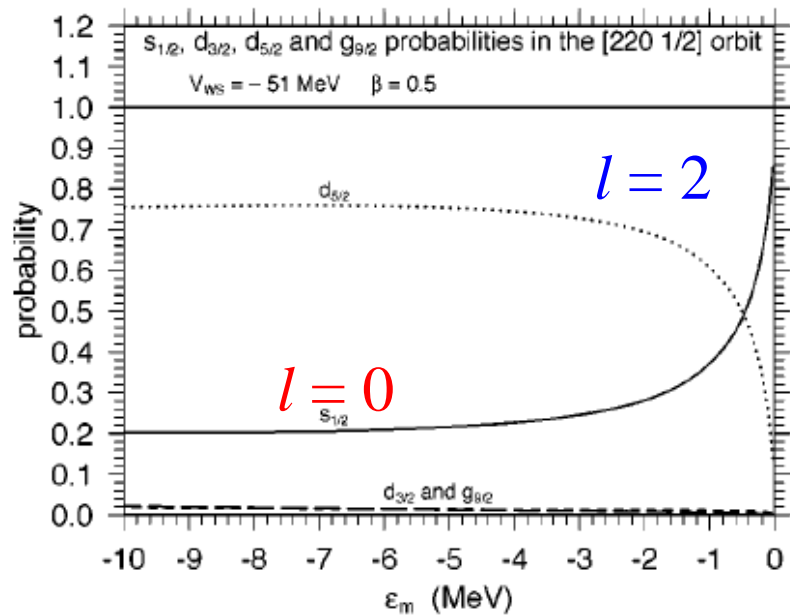
I. Hamamoto, PRC69('04)041306(R)

(enhancement of p -wave component, although not 100% in the zero binding limit)

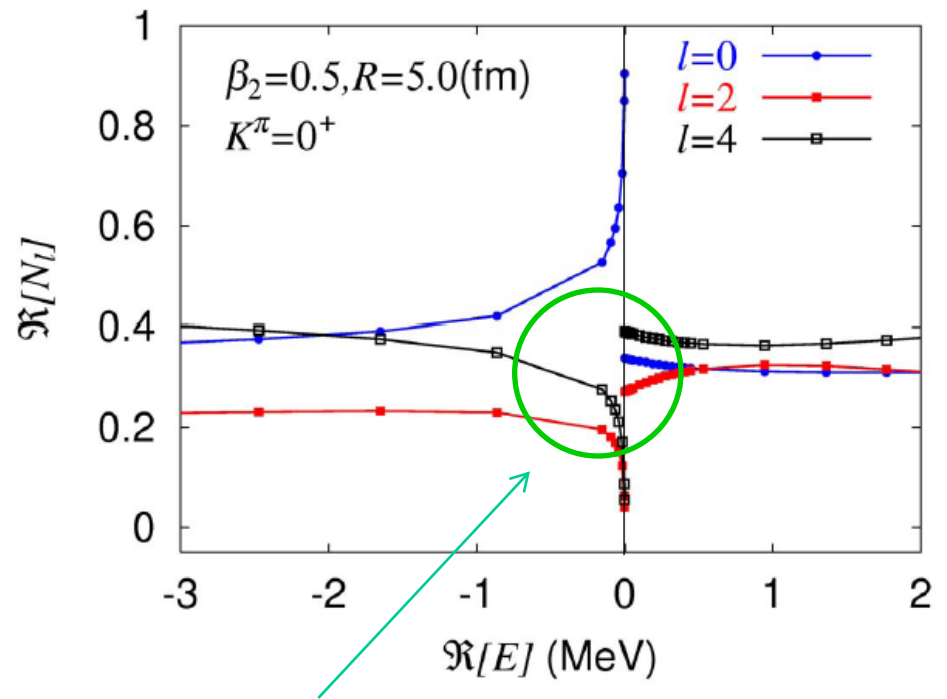
c.f. s -wave dominance and $s.p.$ resonance:

K. Yoshida and K.H., PRC72('05) 064311

c.f. s-wave dominance and s.p. resonance:



I. Hamamoto, PRC69('04)041306(R)



The s-wave dominance phenomenon does not continue to scattering states
 \rightarrow existence of a $K^\pi = 0^+$ resonance

K. Yoshida and K. Hagino,
 PRC72('05)064311

particle-rotor model

Nilsson model: intrinsic (body-fixed) frame formalism

—————→ transformation to the lab. frame

- ✓ angular momentum projection
- ✓ particle-rotor model

For an axially symmetric rotor,

Nilsson: adiabatic (strong coupling) limit of particle-rotor model



core + neutron two-body model
with core excitations

$$\Psi_{IM} = \sum_{I_c, j, l} \left(\begin{array}{c} \text{Yellow oval labeled } I_c \\ \text{Red dot labeled } j, l \\ \text{Line connecting } I_c \text{ and } j, l \end{array} \right)^{(IM)} = \begin{array}{l} |0^+ \otimes p_{3/2}\rangle \\ \text{e.g.,} \\ |2^+ \otimes f_{7/2}\rangle + \dots \end{array}$$

particle-rotor model

Nilsson: adiabatic (strong coupling) limit of particle-rotor model

$$\psi_{IM} = \sum_{I_c, j, l} \left(\text{yellow circle } I_c \text{ with red dot } j, l \right)^{(IM)} = |0^+ \otimes p_{3/2}\rangle + |2^+ \otimes f_{7/2}\rangle + \dots$$

e.g.,

all the members of the ground rotational band are degenerate in energy

→ K : a good quantum number (no Coriolis coupling)



$$\underline{R_{I_c j l}^{(I)}(r)} = A_{j I_c}^{IK} \cdot \underline{\phi_{j l K}(r)}$$

particle-rotor

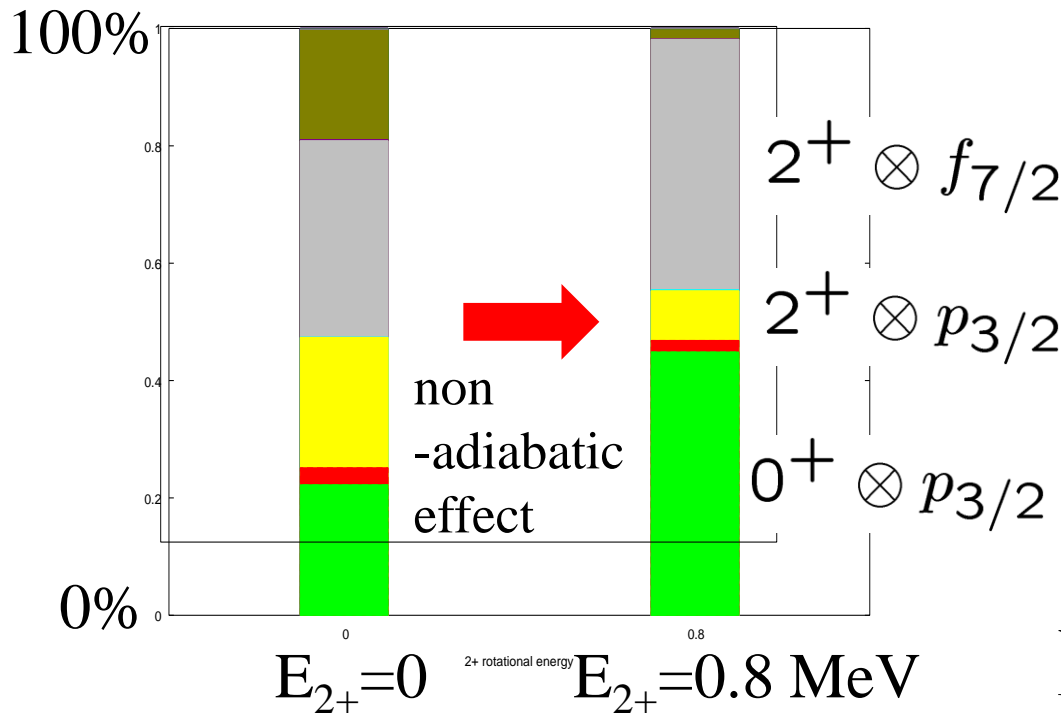
Nilsson

$$A_{j I_c}^{IK} = \sqrt{\frac{2I_c + 1}{2I + 1}} \cdot \sqrt{2} \langle j K I_c 0 | I K \rangle$$

particle-rotor model with finite excitation energy

coupled-channels equations

$$\left(-\frac{\hbar^2}{2m} \frac{d^2}{dr^2} + \frac{l(l+1)\hbar^2}{2mr^2} + V_0(r) + \underbrace{E_{I_c}}_{\text{non-adiabatic effect}} - \epsilon \right) R_{I_c j l}^{(I)}(r) = - \sum_{I'_c, j', l'} \langle [(j l) I_c]^{(IM)} | V_{\text{def}} | [(j' l') I'_c]^{(IM)} \rangle R_{I'_c j' l'}^{(I)}(r)$$



example:

[330 1/2] level at $\beta=0.2$



21st neutron

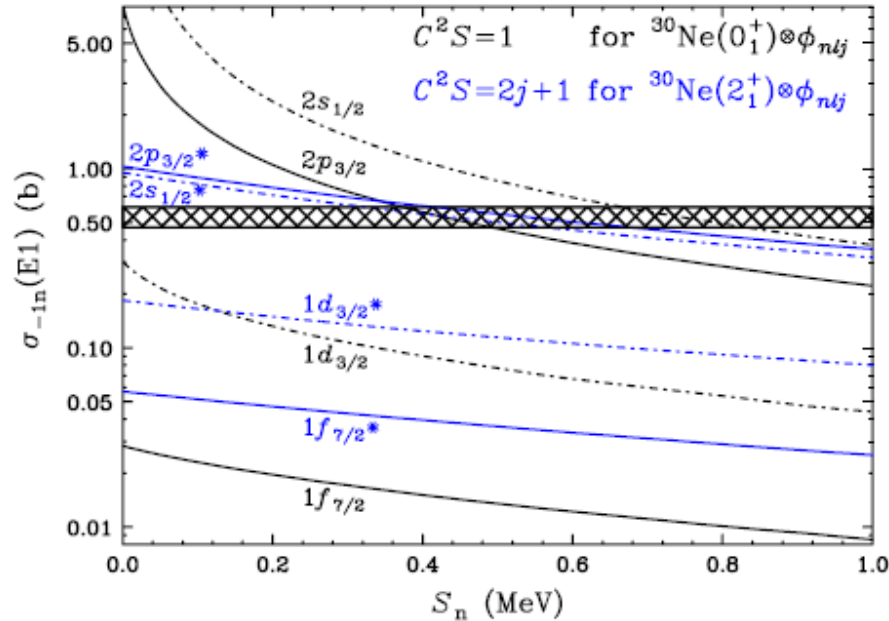
$\epsilon = -0.3$ MeV

spherical basis with
 $R_{\text{box}}=60$ fm

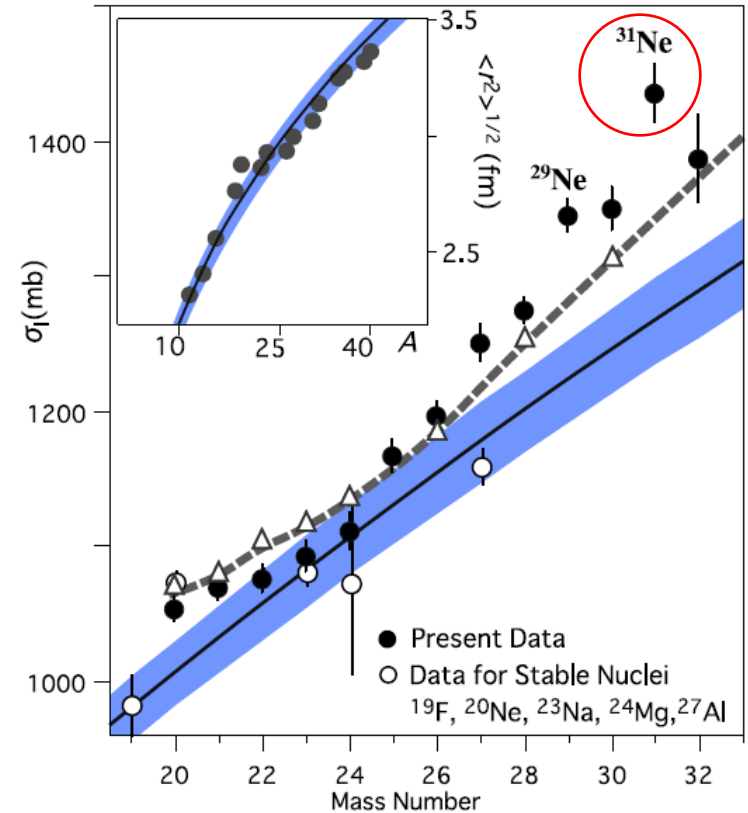
Y. Urata, K.H., and H. Sagawa,
PRC83('11)041303(R)

Application to ^{31}Ne

large Coulomb breakup and interaction cross sections



T. Nakamura et al.,
 PRL103('09)262501

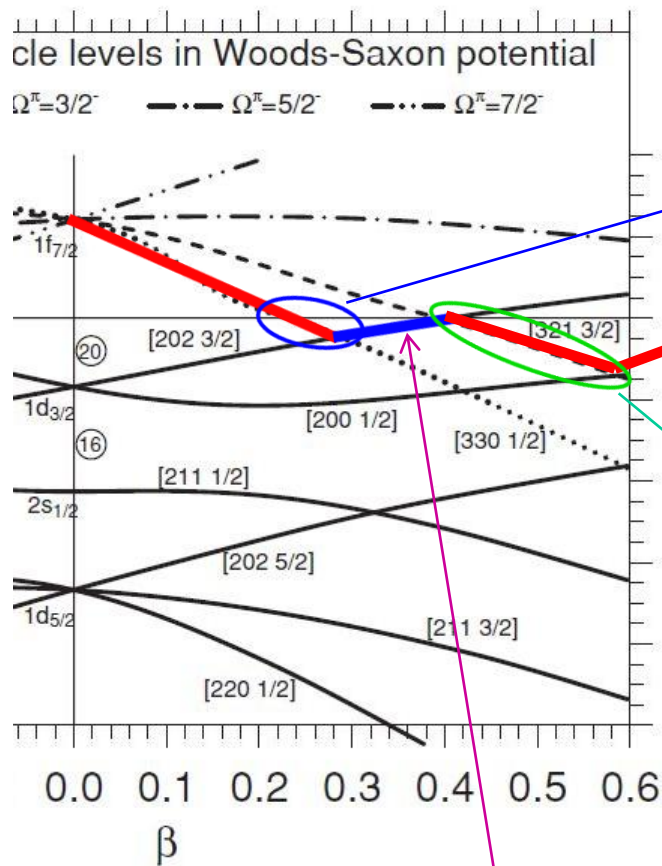


M. Takechi et al., PLB 707('12)357

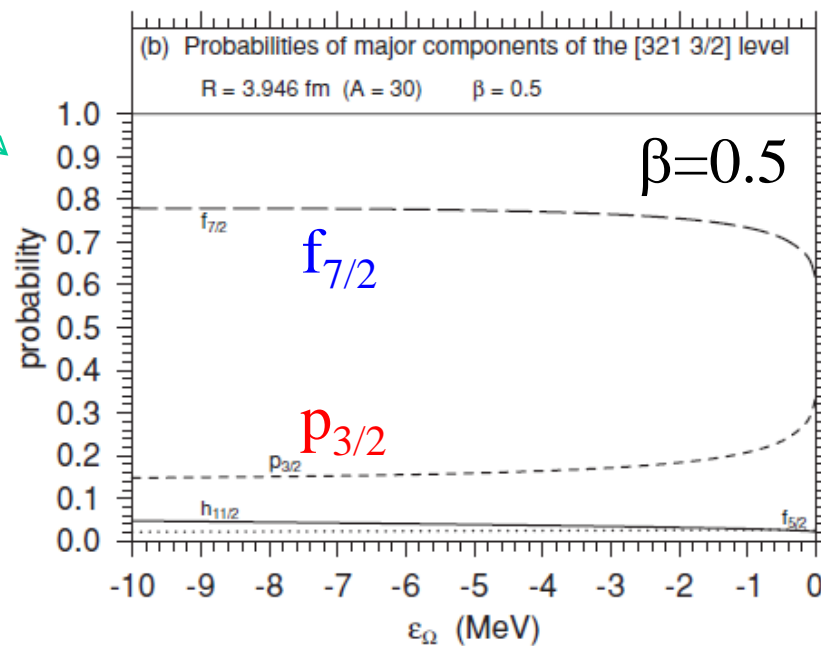
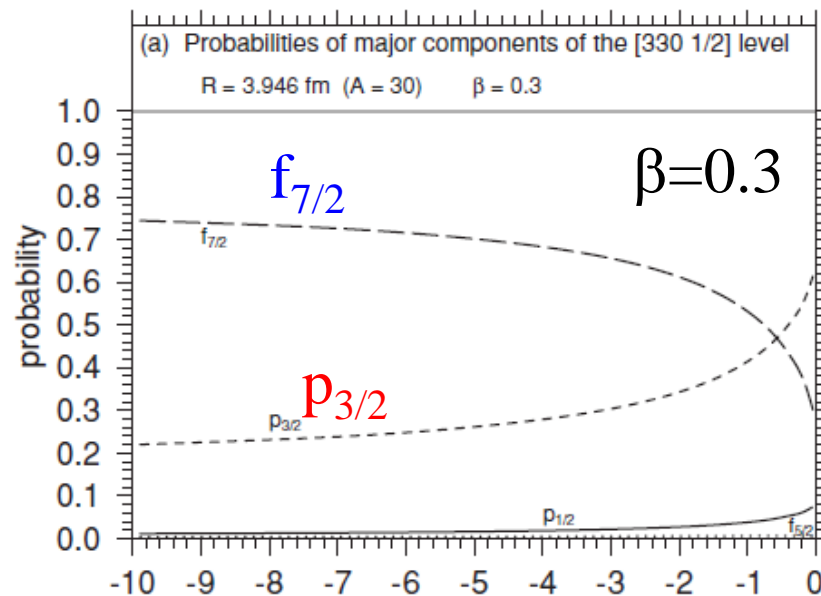
theoretical studies:

- W. Horiuchi et al., PRC81('10)024606
- I. Hamamoto, PRC81('10)021304(R)
- Y. Urata, K.H., H. Sagawa, PRC83('11)041303(R)
- K. Minomo et al., PRL108('12)052503; PRC84('11)034602; PRC85('12)064613

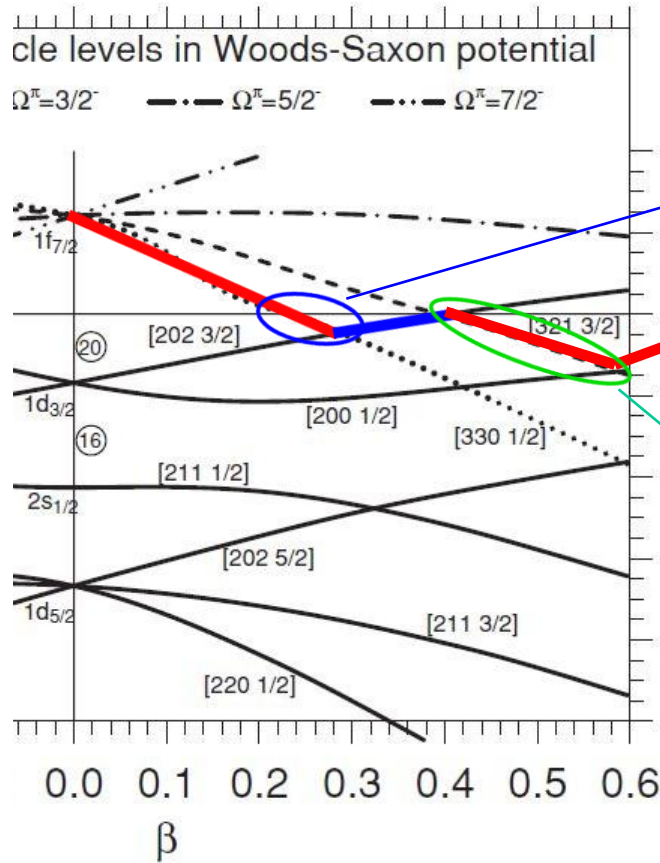
Nilsson model analysis [I. Hamamoto, PRC81('10)021304(R)]



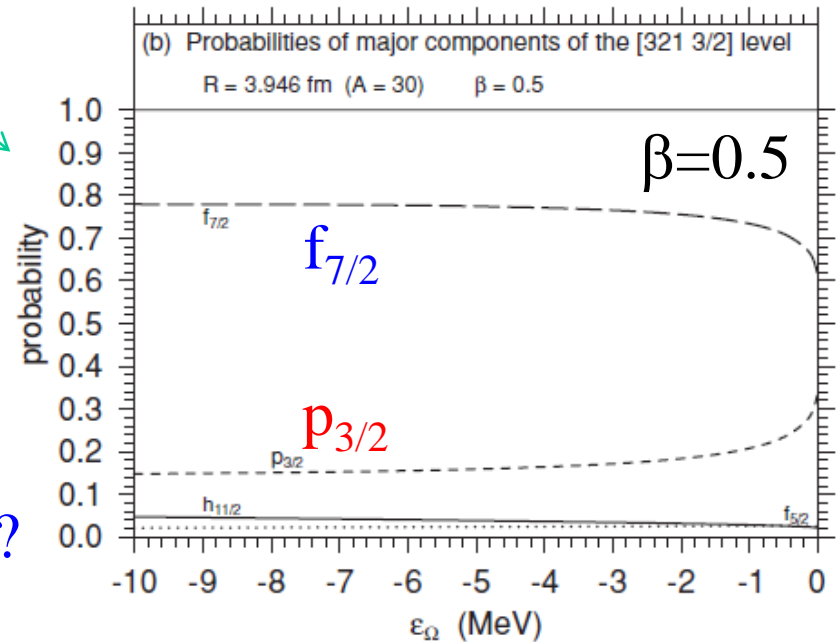
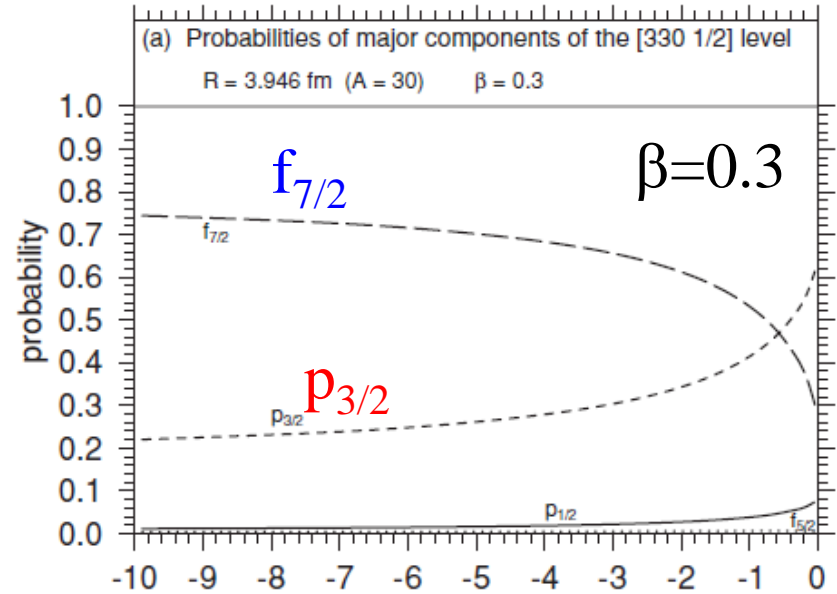
non-halo
($\Omega^\pi = 3/2^+$)



Nilsson model analysis [I. Hamamoto, PRC81('10)021304(R)]

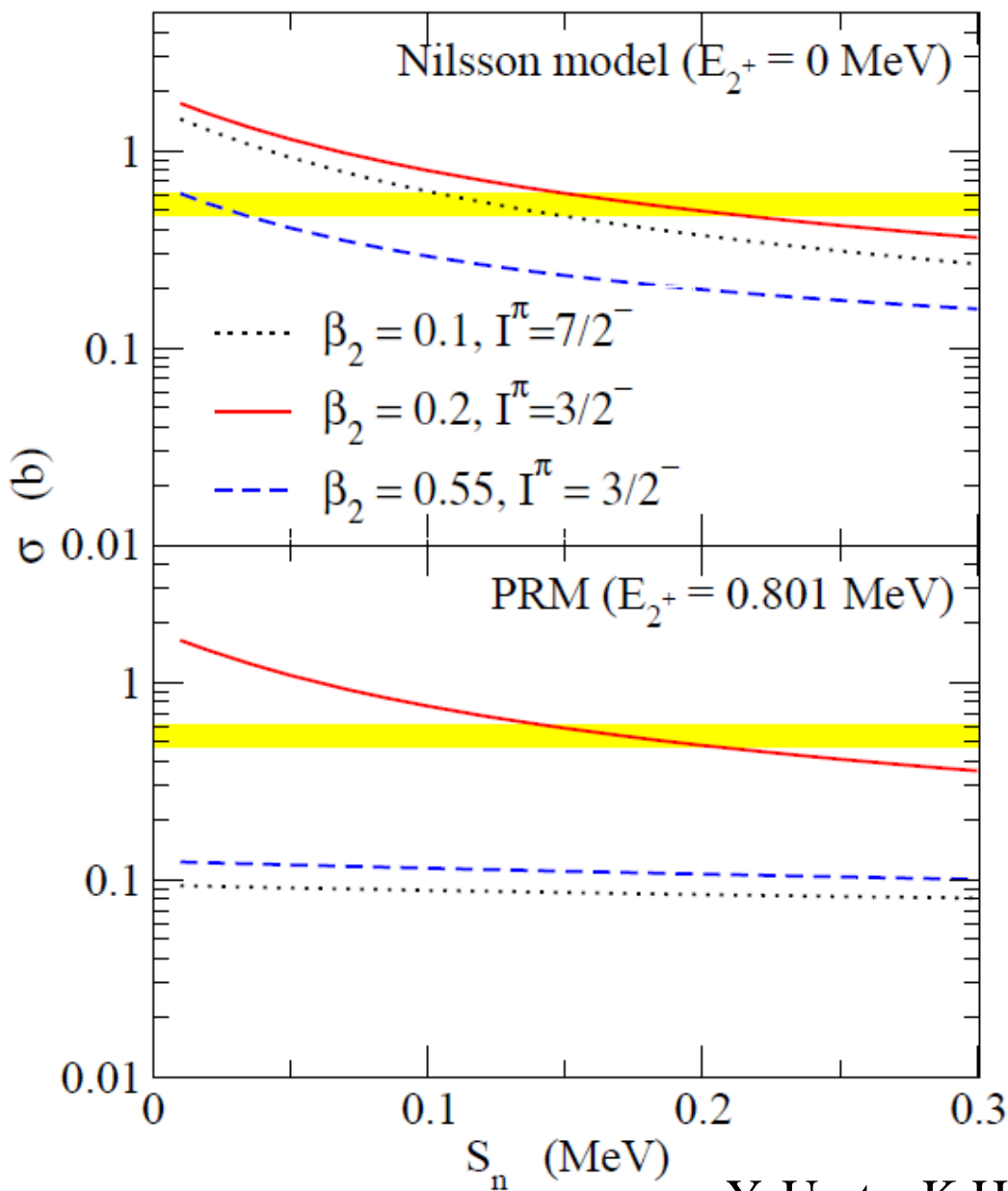


21st
neutron

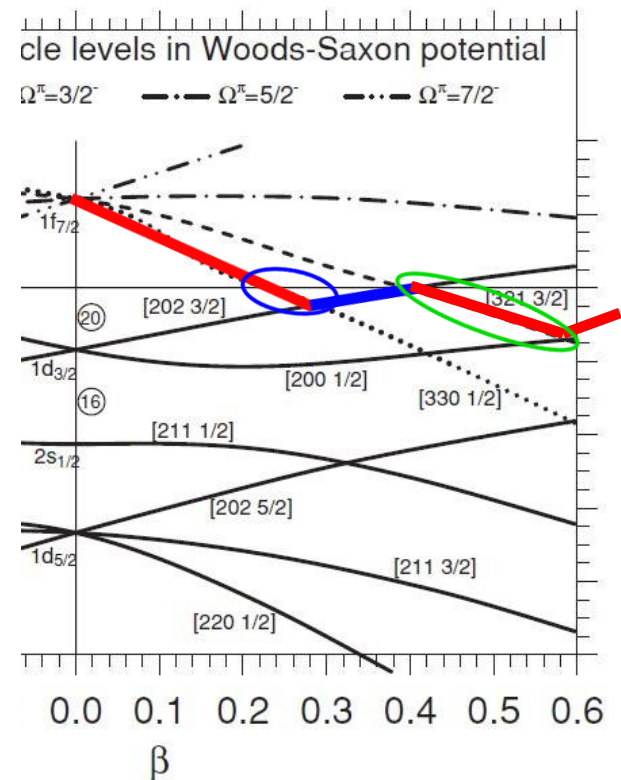


- ◆ non-adiabatic effects?
- ◆ comparison to the data (σ_{bu} and σ_I)?

Coulomb breakup cross sections

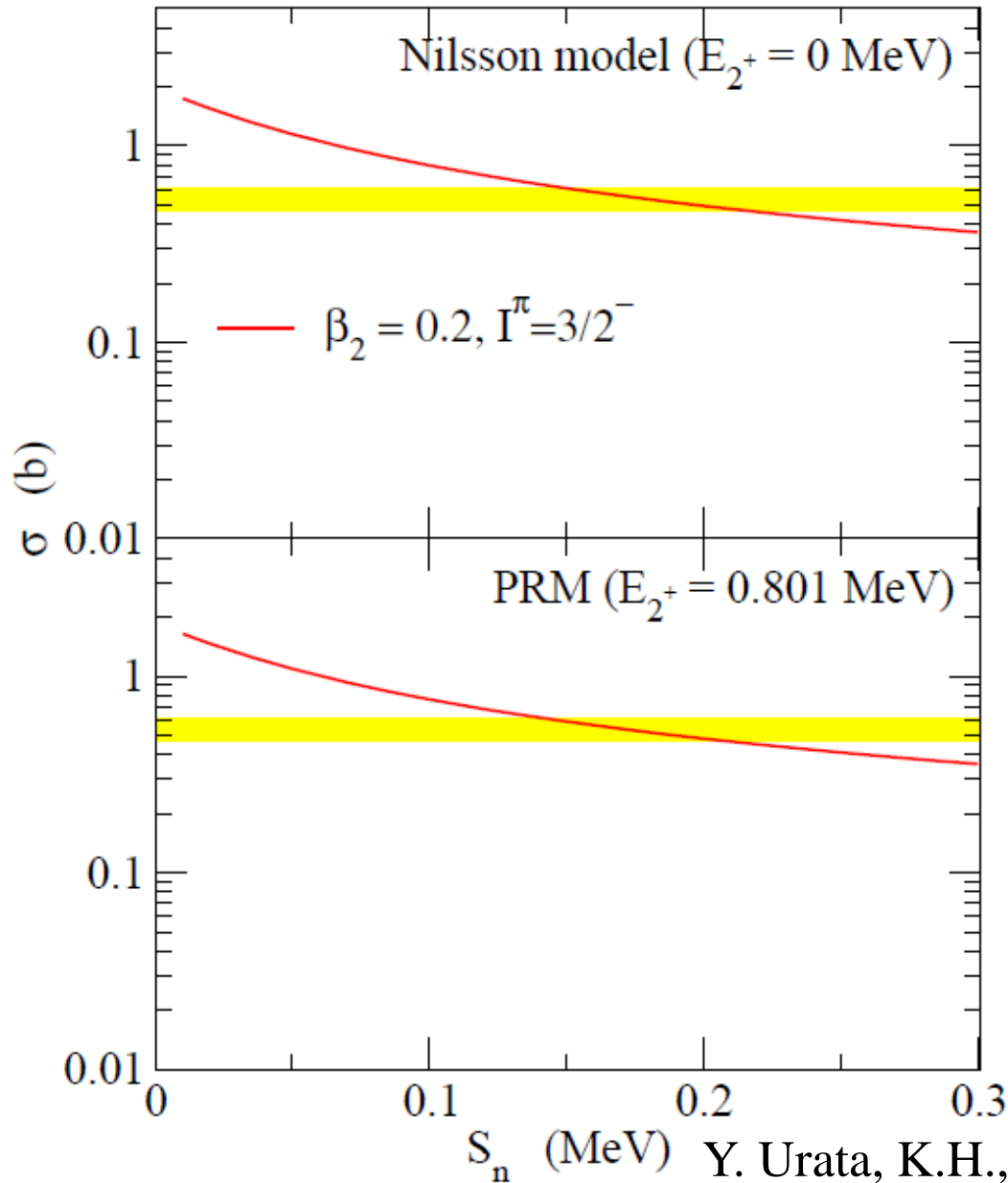


$E_{2^+} (^{30}\text{Ne}) = 0.801(7)$ MeV
 P. Doornenbal et al.,
 PRL103('09)032501
 $S_n (^{31}\text{Ne}) = 0.29 \pm 1.64$ MeV

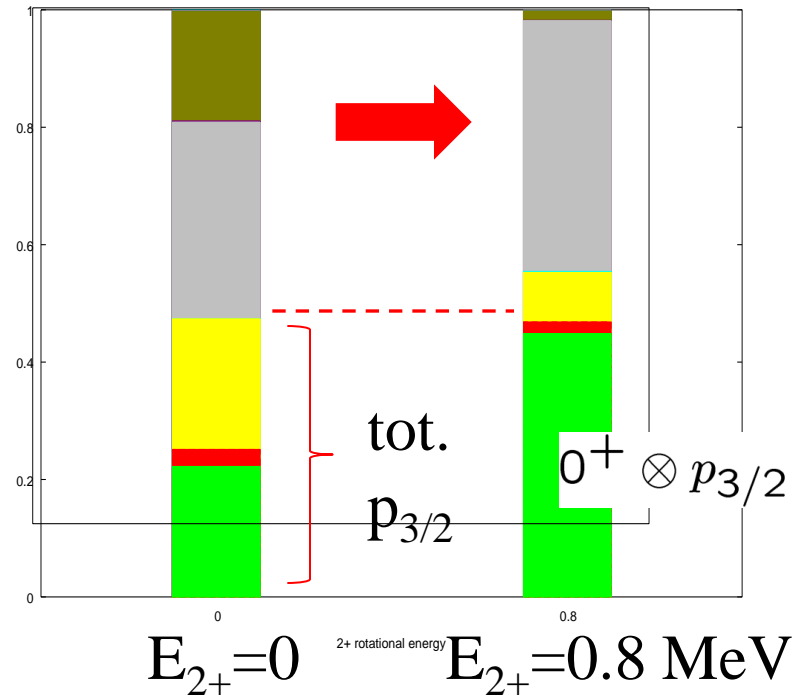


Y. Urata, K.H., and H. Sagawa,
 PRC83('11)041303(R)

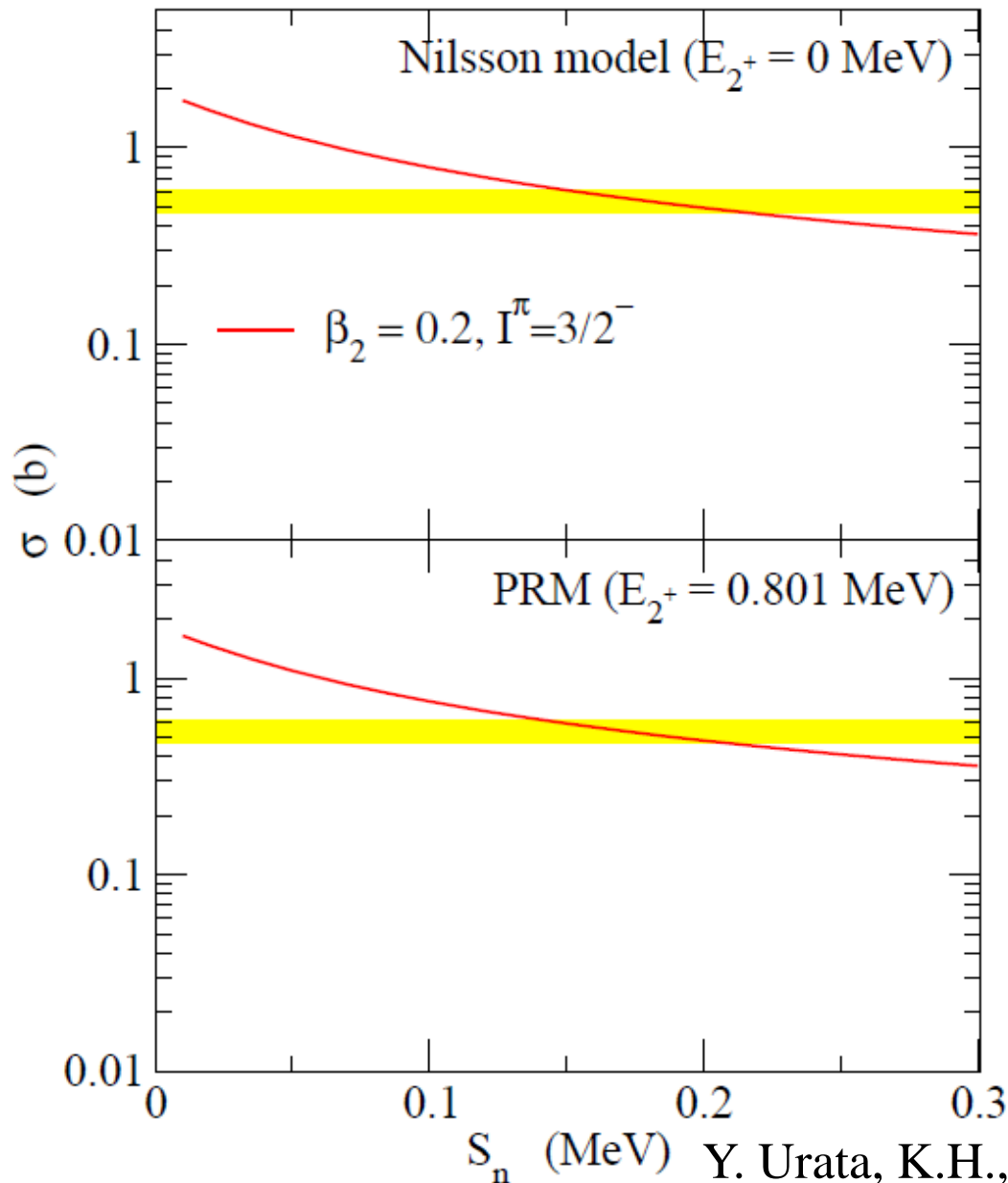
Coulomb breakup cross sections



$\beta \sim 0.2$: small non-adiabatic effects



Coulomb breakup cross sections



↑
Coul.BU

$$\sigma_{\text{bu}}(0^+) = 0.45(11) \text{ b}$$

T. Nakamura et al.,
preliminary data

RPM for $S_n = 0.2$ MeV

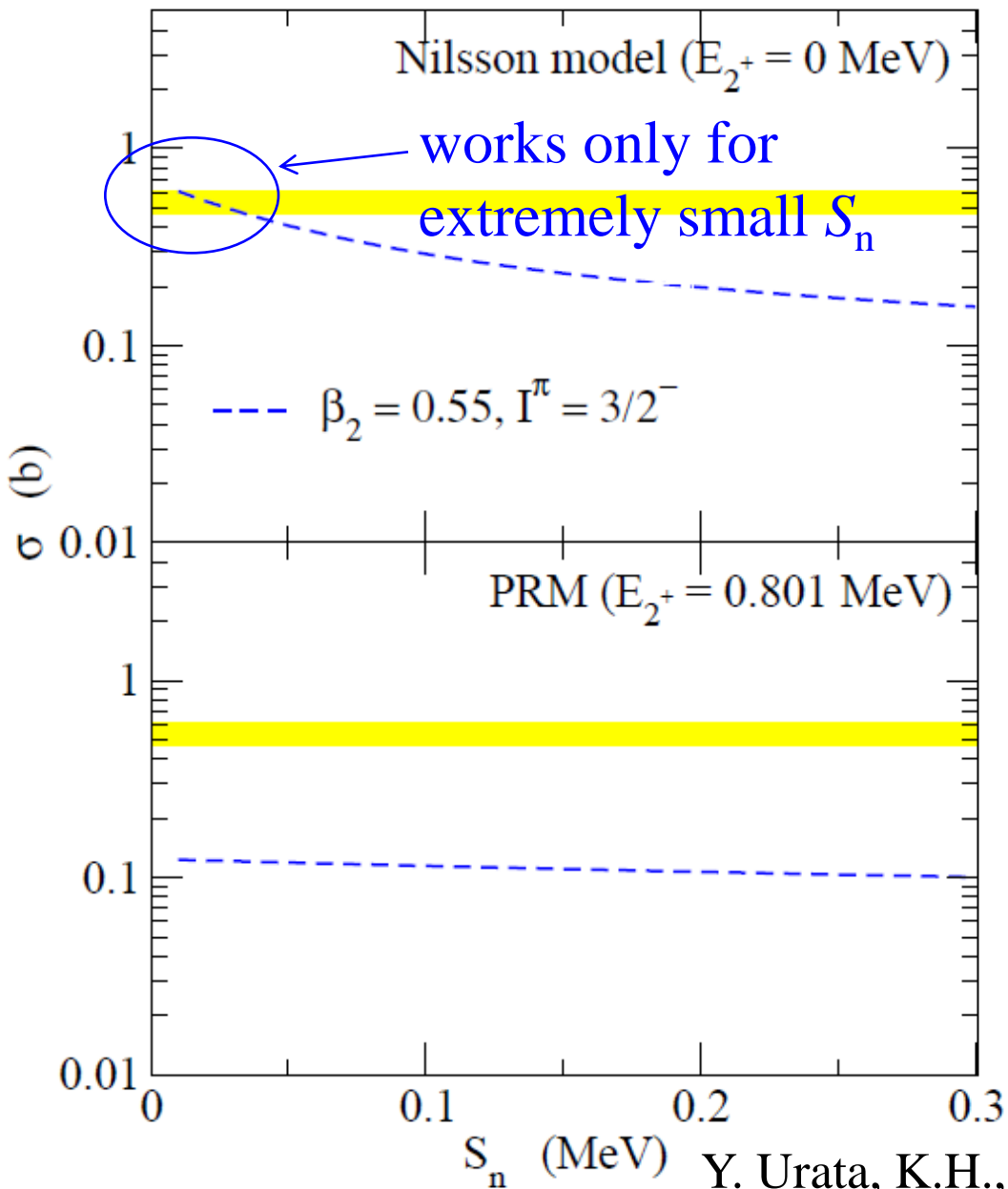
$$\sigma_{\text{bu}}(0^+) = 0.443 \text{ b}$$

good agreement with
the data

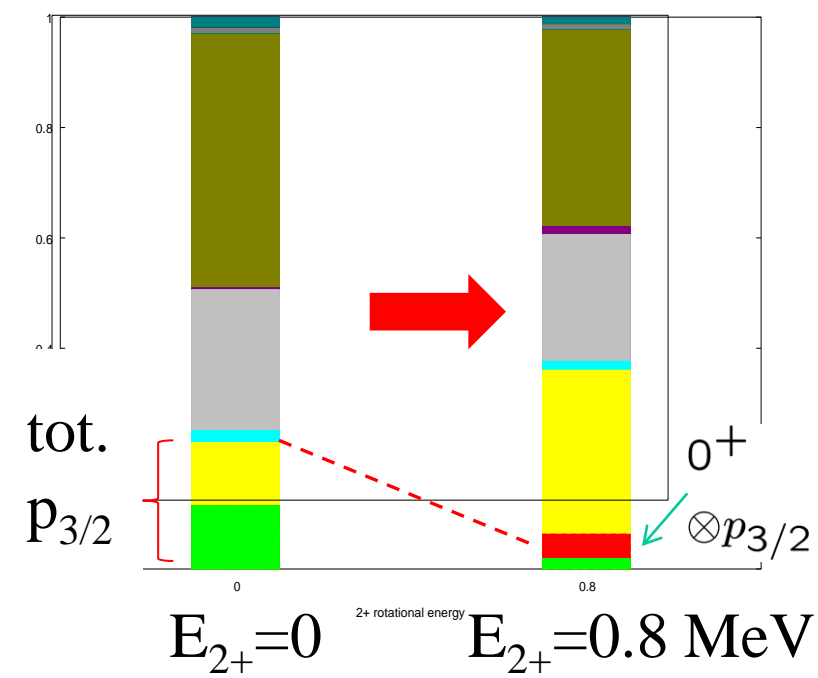
cf. Nilsson: $\sigma_{\text{bu}}(0^+) = 0.216 \text{ b}$

Y. Urata, K.H., and H. Sagawa,
PRC83('11)041303(R)

Coulomb breakup cross sections



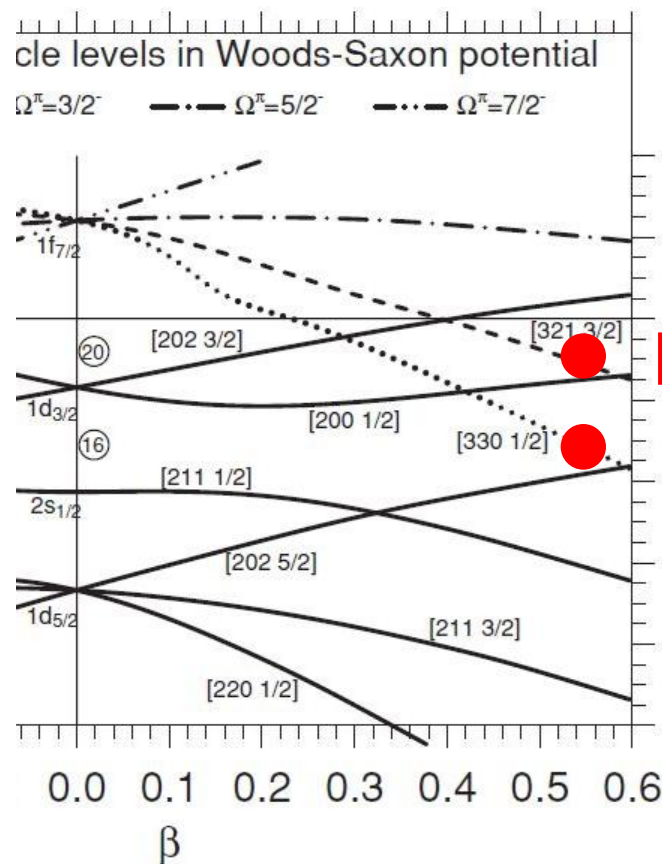
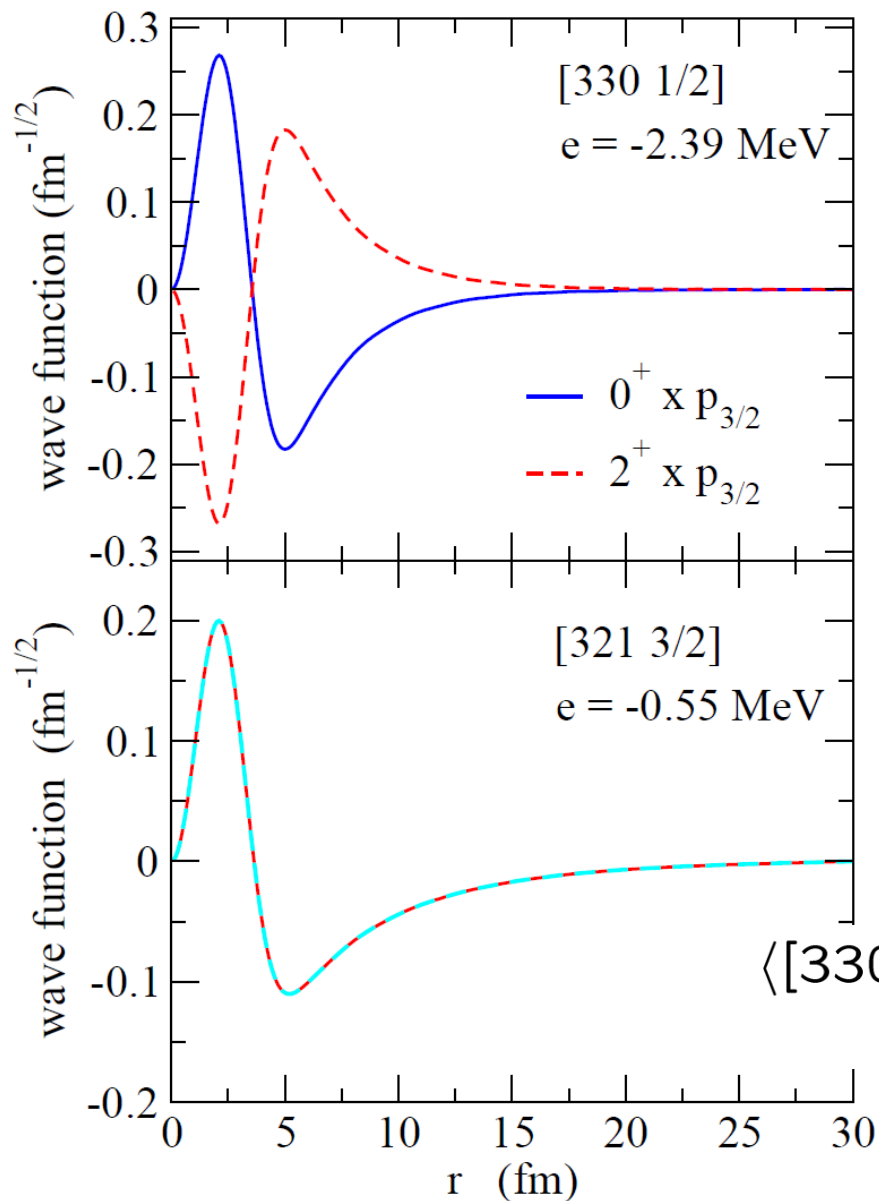
$\beta \sim 0.55$: large non-adiabatic effects



Y. Urata, K.H., and H. Sagawa,
PRC83('11)041303(R)

two-level mixing between [330 1/2] and [321 3/2]

$I^\pi = 3/2^-$ at $\beta=0.55$

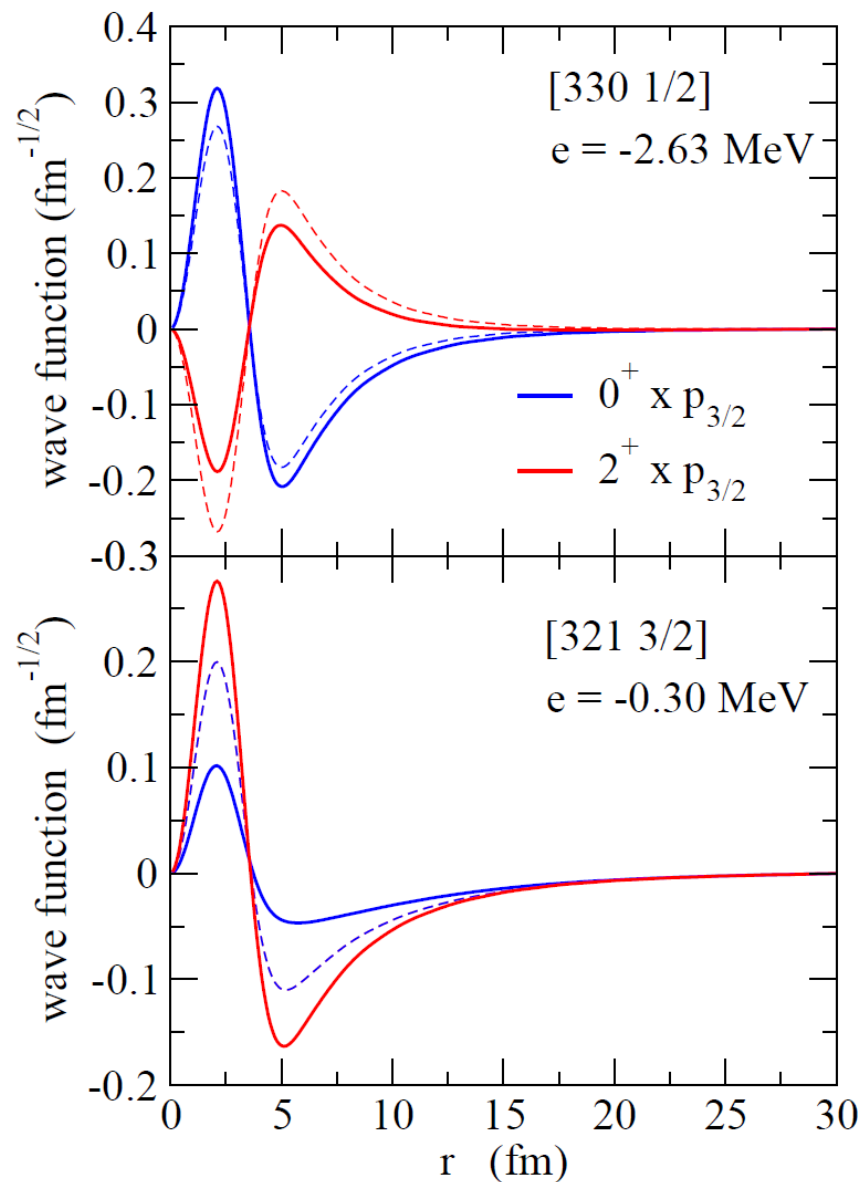


$$\langle [330\ 1/2]^{(I=3/2)} | H_{\text{rot}} | [321\ 3/2]^{(I=3/2)} \rangle = -0.718\text{ MeV}$$

for $E(2^+) = 0.8\text{ MeV}$

$$\langle [330 \ 1/2] | H_{\text{rot}} | [321 \ 3/2] \rangle \longrightarrow \text{diagonalize} \begin{pmatrix} -2.38 & -0.718 \\ -0.718 & -0.547 \end{pmatrix}$$

$$= -0.718 \text{ MeV}$$



$$0.95|[330 \ 1/2]\rangle + 0.33|[321 \ 3/2]\rangle$$

$$0^+ \times p_{3/2}: 19.4\% \rightarrow 27.1\%$$

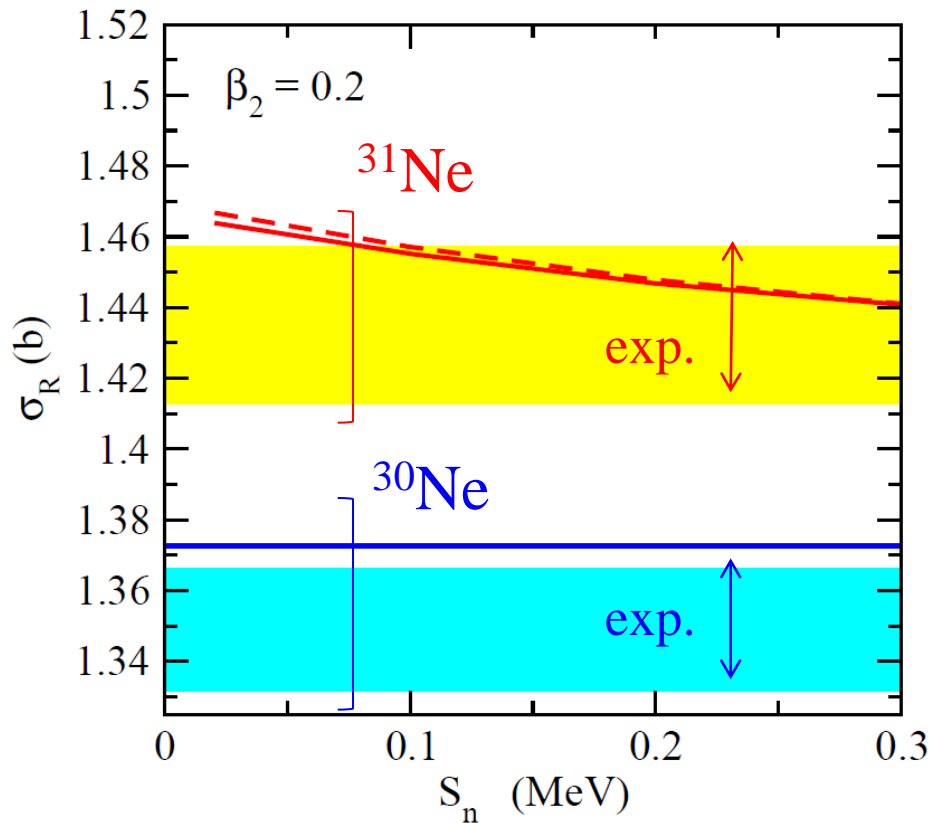
$$2^+ \times p_{3/2}: 19.4\% \rightarrow 9.85\%$$

$$0.95|[321 \ 3/2]\rangle - 0.33|[330 \ 1/2]\rangle$$

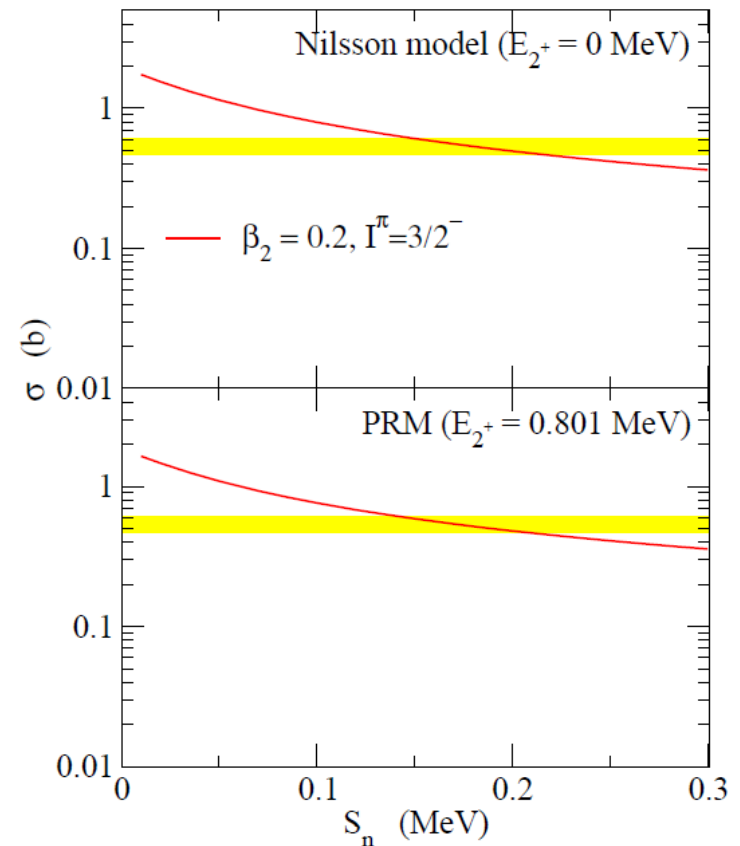
$$0^+ \times p_{3/2}: 10.5\% \rightarrow 2.82\%$$

$$2^+ \times p_{3/2}: 10.5\% \rightarrow 20.1\%$$

Reaction cross section

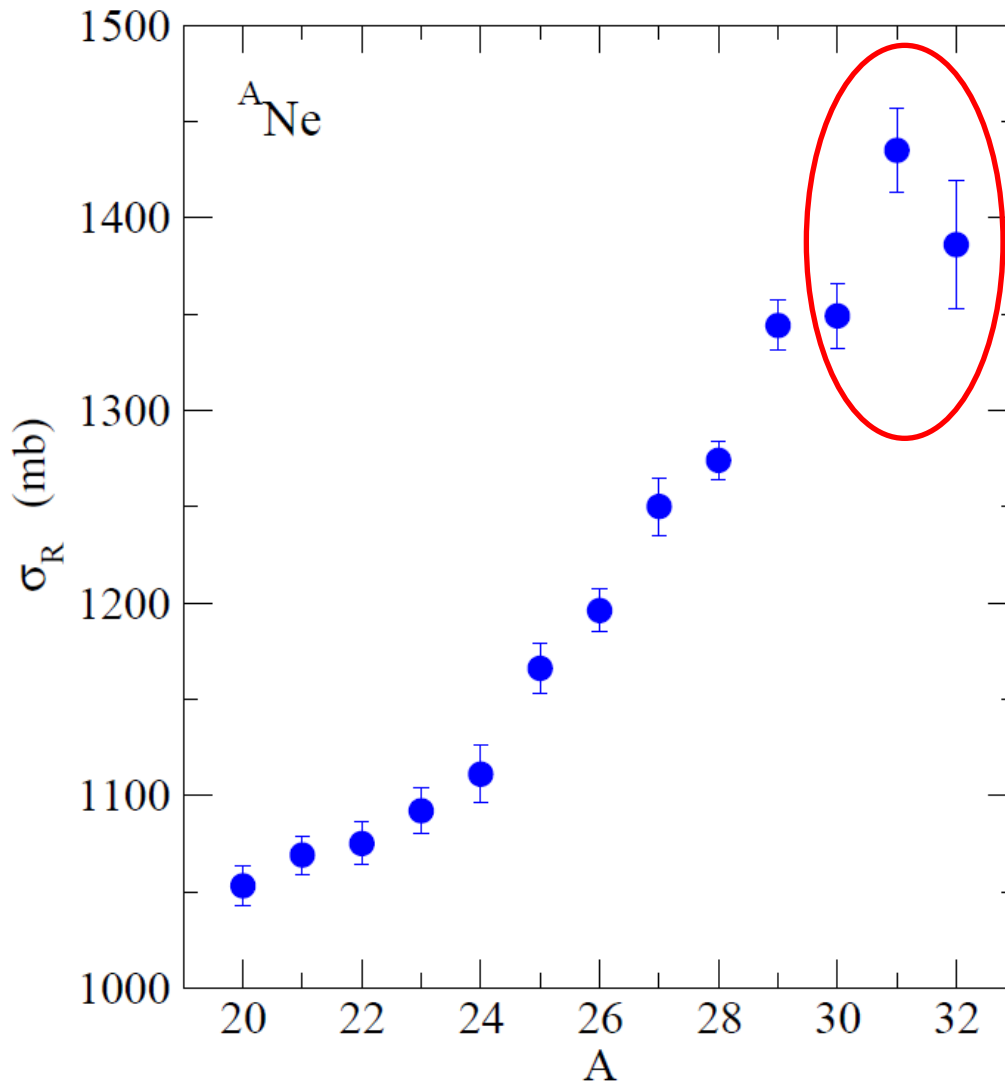


$I^\pi = 3/2^-$ at $\beta \sim 0.2$:
consistent both with σ_{bu} and σ_R



Odd-even staggering of interaction cross sections

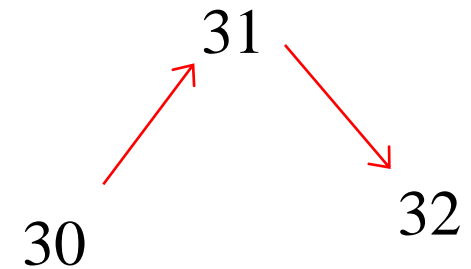
σ_I of unstable nuclei: often show a large odd-even staggering



Typical example:

Recent experimental data
on Ne isotopes

M. Takechi et al.,
Phys. Lett. B707 ('12) 357



clear odd-even effect

- deformation effect?
- pairing effect?

➤ pairing anti-halo effect

K. Bennaceur, J. Dobaczewski,
and M. Ploszajczak,
PLB496('00)154

pairing



asymptotic behavior of s.p.
wave functions



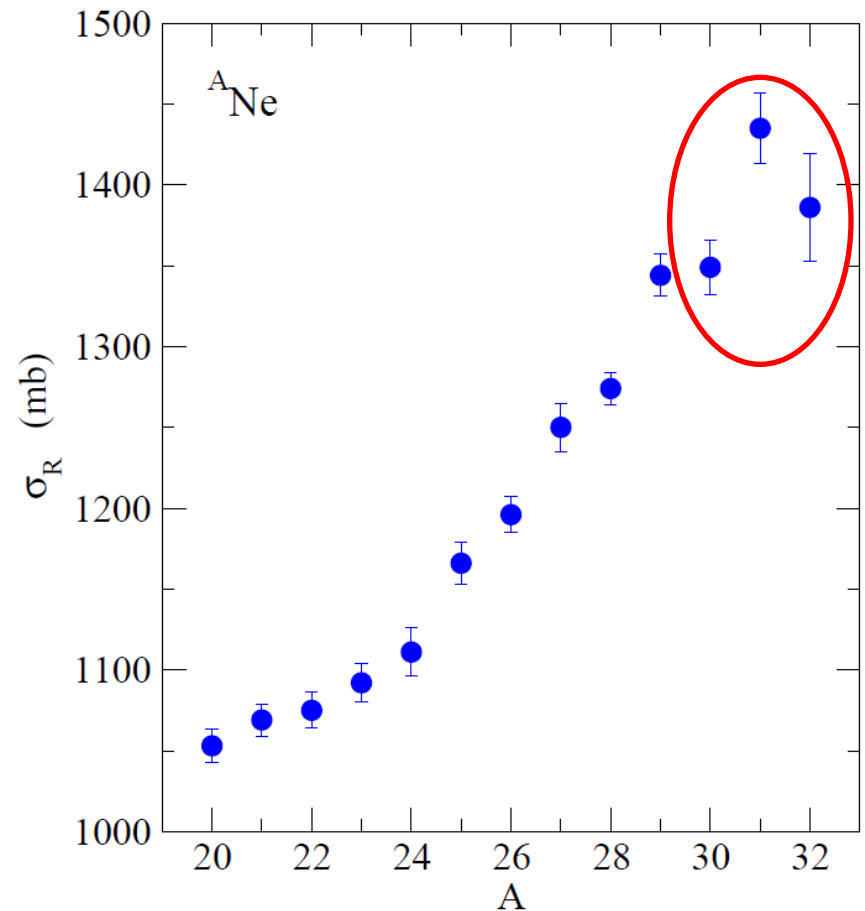
suppression of density distribution

Our motivation:

Relation between the odd-mass staggering (OES) of σ_R
and pairing (anti-halo) effect?

First experimental evidence for the anti-halo effect?

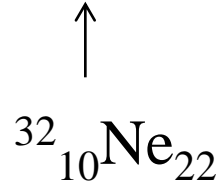
➤ odd-even staggering of σ_R



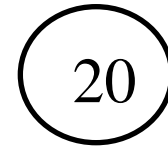
Model: HFB with a Woods-Saxon mean-field potential

$$\begin{pmatrix} \hat{h} - \lambda & \Delta(r) \\ \Delta(r) & -\hat{h} + \lambda \end{pmatrix} \begin{pmatrix} U_k(r) \\ V_k(r) \end{pmatrix} = E_k \begin{pmatrix} U_k(r) \\ V_k(r) \end{pmatrix}$$

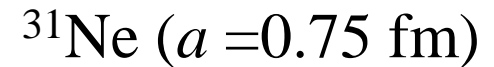
$$\hat{h} = -\frac{\hbar^2}{2m} \nabla^2 + V_{\text{WS}}(r)$$



-0.066 MeV ——— 1f_{7/2}
-0.321 MeV ——— 2p_{3/2}



$$\Delta(r) = \frac{V_{\text{pair}}}{2} \left(1 - \frac{\rho(r)}{\rho_0} \right) \tilde{\rho}_n(r)$$



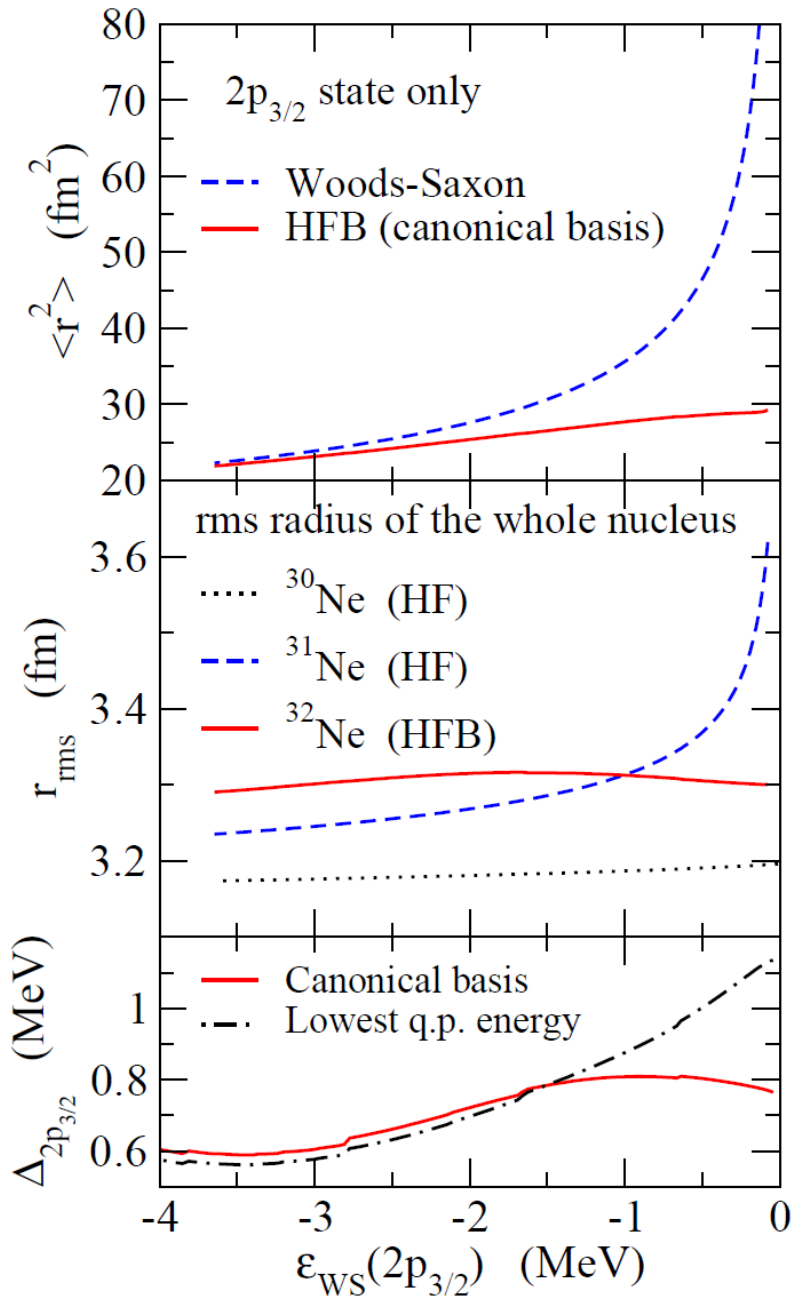
$$\tilde{\rho}_n(r) = - \sum_{k=n} U_k^*(\mathbf{r}) V_k(\mathbf{r})$$

✓ λ : self-consistently determined so that $N=22$

✓ $E_{\text{cut}} = 30 \text{ MeV}$ above λ

✓ $R_{\text{box}} = 60 \text{ fm}$

rms radius and pairing gap



suppression of the radius

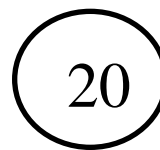


the effective pairing gap persists for both the definitions

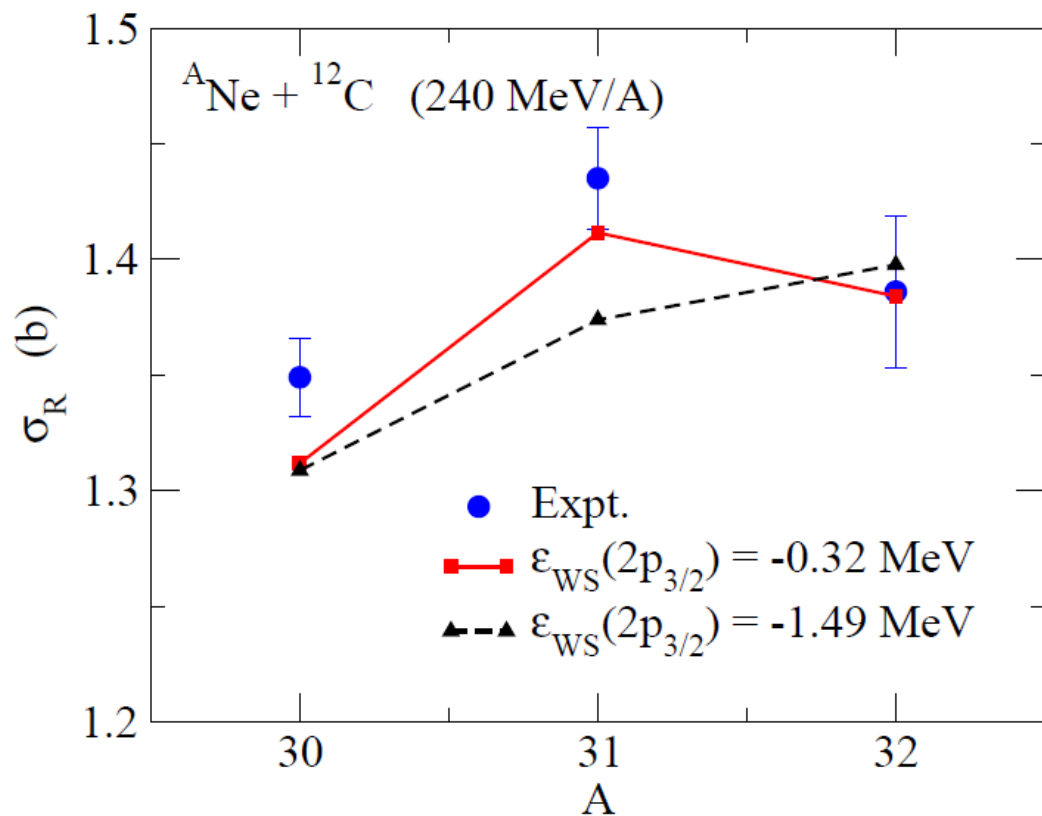
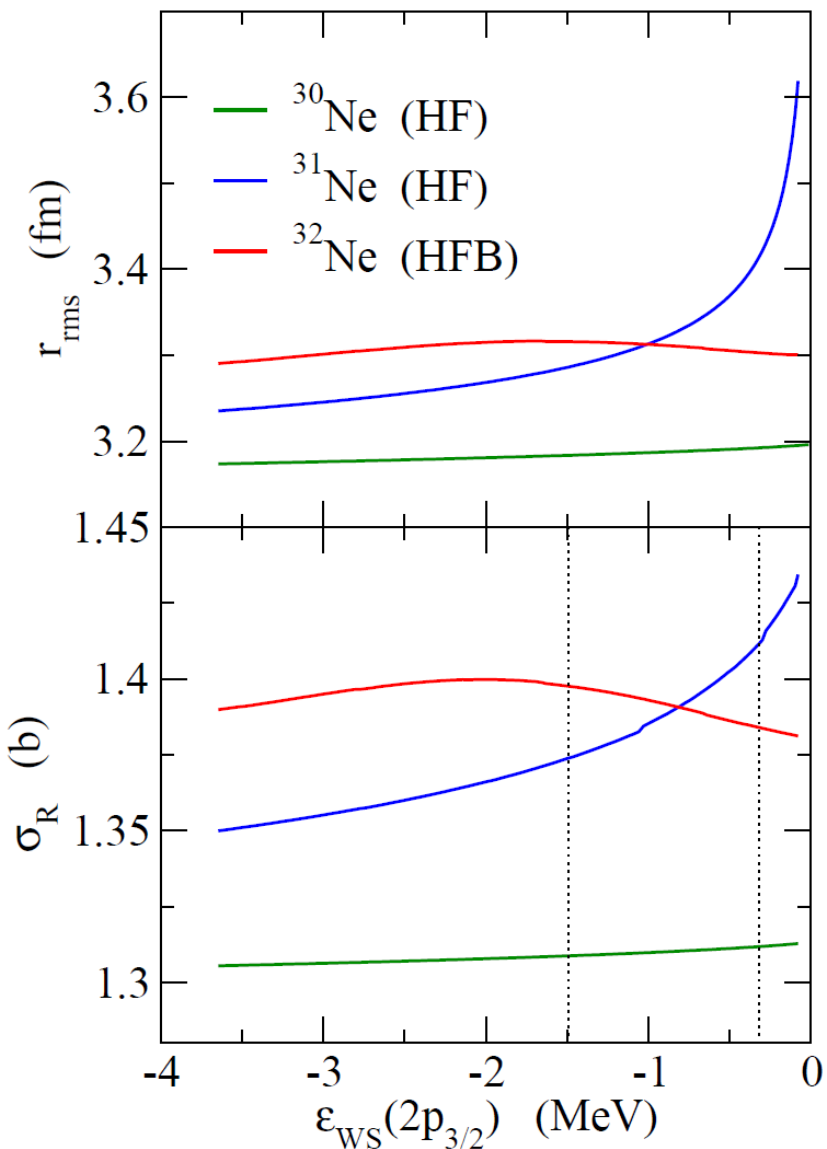
rms radius and reaction cross section

HFB with a spherical Woods-Saxon

-0.066 MeV ——— $1f_{7/2}$
-0.321 MeV ——— $2p_{3/2}$



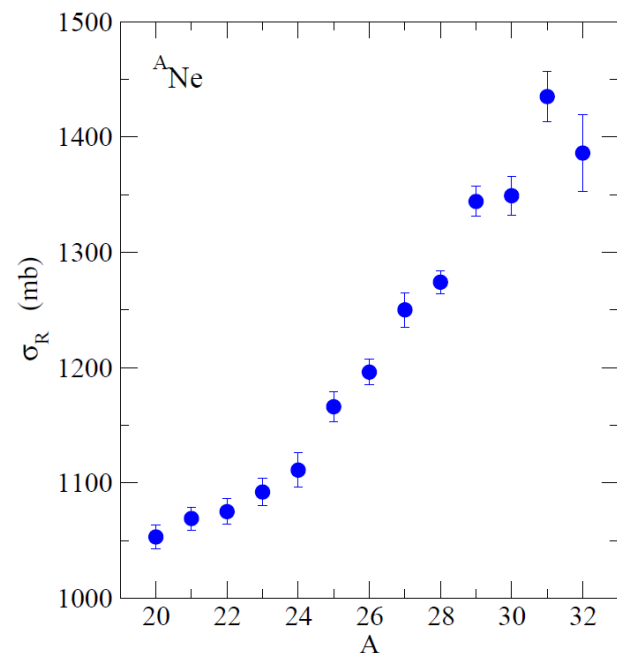
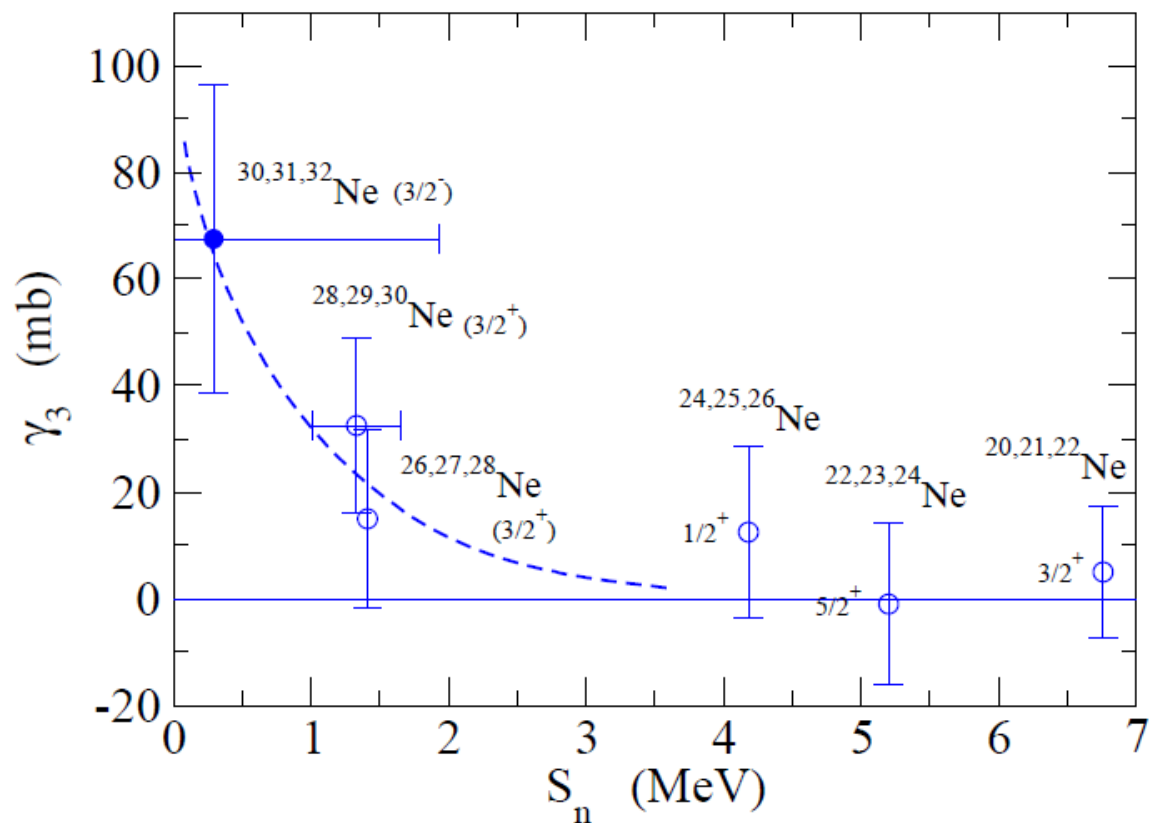
^{31}Ne ($a = 0.75$ fm)



Systematics

OES parameter

$$\gamma_3 \equiv -\frac{1}{2}[\sigma_R(A+2) - 2\sigma_R(A+1) + \sigma_R(A)]$$



Summary and Discussions

deformation \longrightarrow mixture of angular momenta
 \longrightarrow enlarges a possibility of halo formation

□ good example: ^{31}Ne

$0^+ \times p_{3/2}$: 44.9 %

$2^+ \times p_{3/2}$: 8.4 %

$2^+ \times f_{7/2}$: 42.7 %

\longleftarrow non-adiabatic particle-rotor model
with $\beta \sim 0.2$

\longrightarrow well accounts for $\sigma_{\text{C-bu}}(\text{tot})$, $\sigma_{\text{C-bu}}(0^+)$, and σ_{R} simultaneously

□ Odd-even staggering of σ_{R}

✓ an important role of pairing correlation

✓ OES parameter: a good tool to investigate the pairing correlation

✓ role of deformation? \longleftarrow deformed HFB (a work in progress)

Summary and Discussions

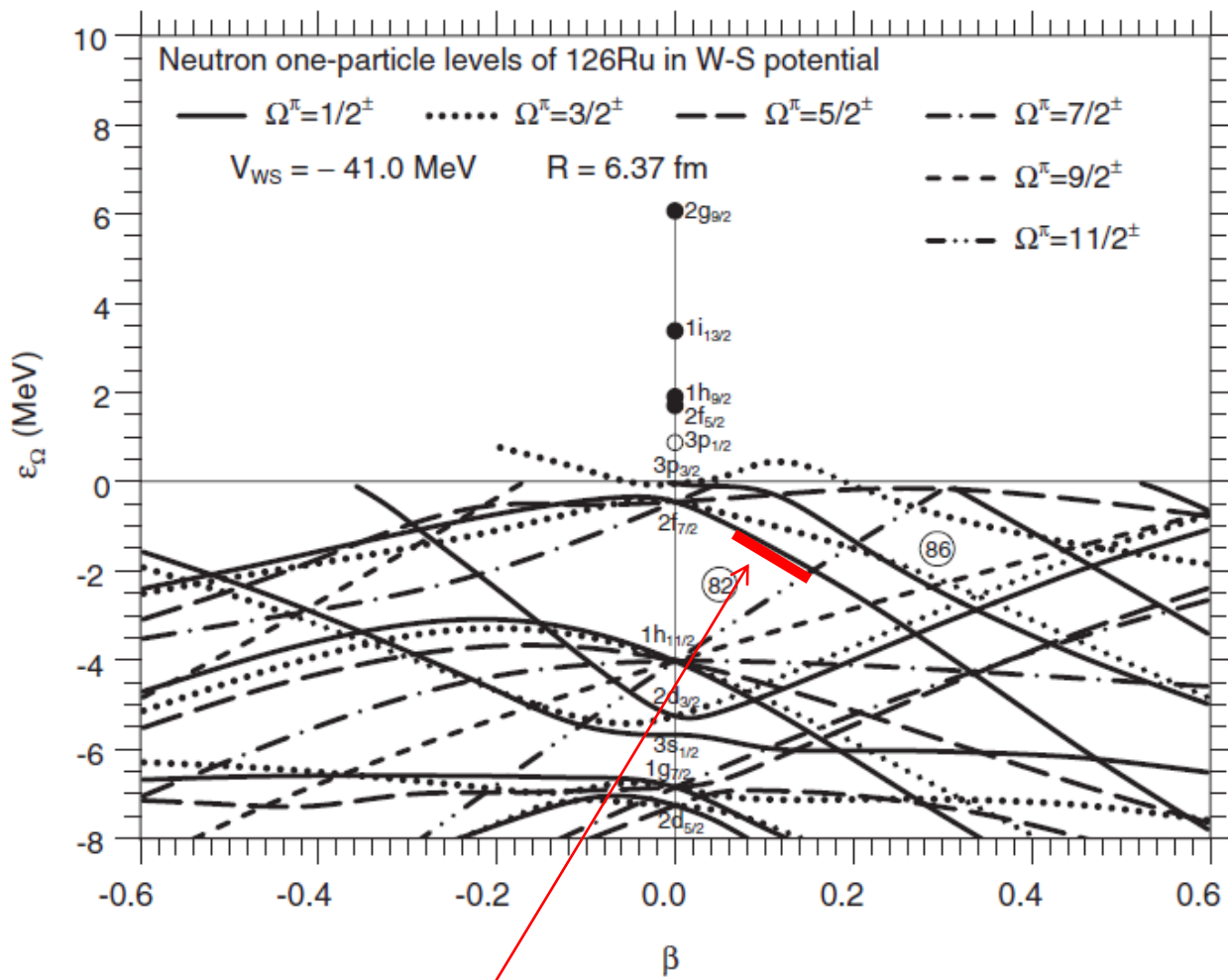
deformation \longrightarrow mixture of angular momenta
 \longrightarrow enlarges a possibility of halo formation

□ good example: ^{31}Ne

Other candidates?

^{19}C	}	I. Hamamoto, PRC76('07)054319	
$^{33,35,37}\text{Mg}$			
$^{43,45}\text{S}$			I. Hamamoto, PRC79('09)014307
^{127}Ru			I. Hamamoto, PRC85('12)064329

$^{126}_{44}\text{Ru}_{83}$



$\Omega^\pi = 1/2^-$

cf. Skyrme-HFB: $\beta = 0$

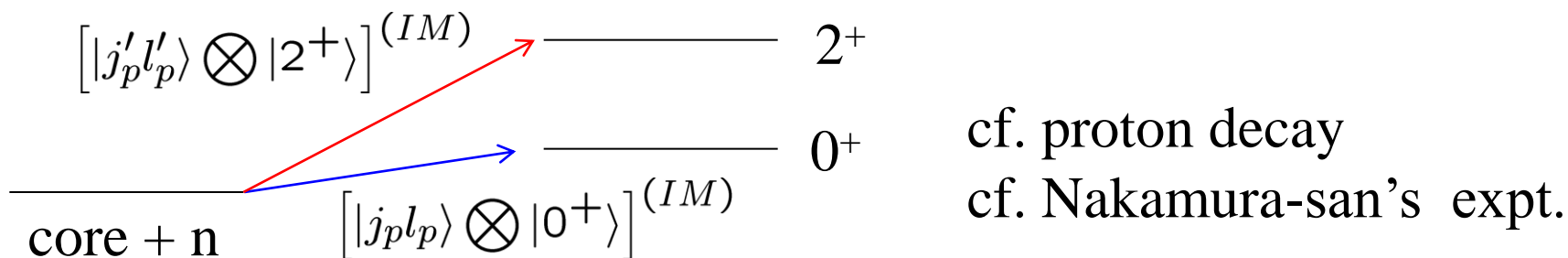
Perspectives: deformed halo nuclei

✓ Possibility of a heavy halo nucleus

what is the heaviest halo nucleus?

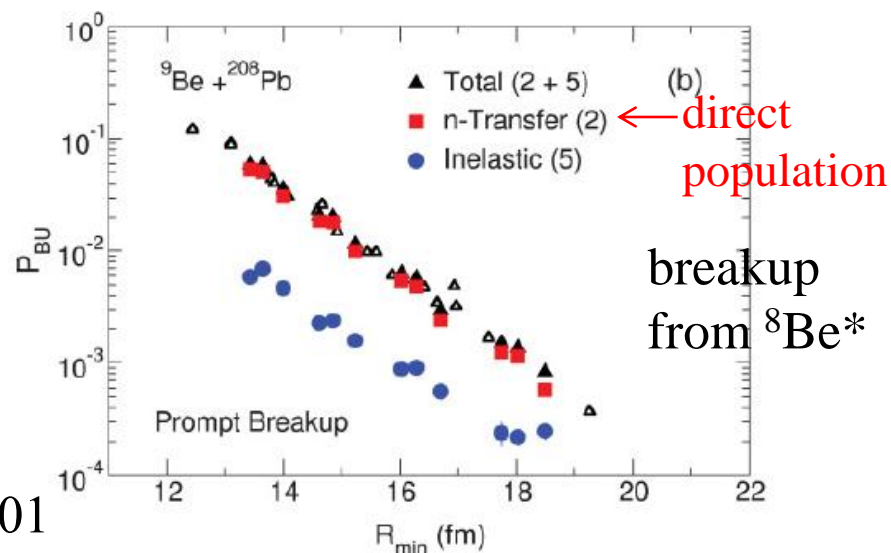
✓ “Fine structure” in breakup/transfer reactions

direct population of the 2^+ state after breakup/transfer



✓ Influence on low-energy heavy-ion reactions (e.g., subbarrier fusion)

interplay between
breakup/ transfer/ rotational
couplings



R. Rafiei et al.,
PRC81('10)024601